

Quantum statistical properties of multiphoton hypergeometric coherent states and the discrete circle representation

S. Arjika

*Department of Mathematics and Computers Sciences, University of Agadez, Niger**

M. Calixto

*Department of Applied Mathematics and Institute Carlos I of Theoretical and Computational Physics,
University of Granada, Fuentenueva s/n, 18071 Granada, Spain†*

J. Guerrero

*Department of Mathematics, University of Jaen,
Campus Las Lagunillas s/n, 23071 Jaen, Spain‡*

(Dated: January 18, 2022)

We review the definition of hypergeometric coherent states, discussing some representative examples. Then we study mathematical and statistical properties of hypergeometric Schrödinger cat states, defined as orthonormalized eigenstates of k -th powers of nonlinear f -oscillator annihilation operators, with f of hypergeometric type. These “ k -hypercats” can be written as an equally weighted superposition of hypergeometric coherent states $|z_l\rangle, l = 0, 1, \dots, k-1$, with $z_l = ze^{2\pi il/k}$ a k -th root of z^k , and they interpolate between number and coherent states. This fact motivates a continuous circle representation for high k . We also extend our study to truncated hypergeometric functions (finite dimensional Hilbert spaces) and a discrete exact circle representation is provided. We also show how to generate k -hypercats by amplitude dispersion in a Kerr medium and analyze their generalized Husimi Q -function in the super- and sub-Poissonian cases at different fractions of the revival time.

Keywords: nonlinear, nonclassical, macroscopic superpositions of quantum states, generalized even/odd states, multicomponent Schrödinger cat states, multiphoton or circular states.

MSC: 81R30

I. INTRODUCTION

The subject of Coherent States (CS) is traced back to 1926 when Schrödinger first introduced the notion of (canonical) CS of the harmonic oscillator [1]. Later, R. Glauber [2] realized the importance of CS in the description of the radiation field. Since then, the subject of CS has grown and pervades almost all branches of quantum physics (see e.g. [3, 4] and [5, 6] for old and recent reviews and [7–11] for standard textbooks). Besides, some other important topics in applied mathematics, like the theory of wavelets, are also related to the notion of CS [12]. Standard (canonical) CS have been generalized in many ways. For example, in 1972, Gilmore [13, 14] and Perelomov [8, 15] realized that canonical CS were rooted in group theory (the Heisenberg-Weyl group) and generalized the notion of CS by extending the concept of displacement operator $D(z) = \exp(z\hat{a} - \bar{z}\hat{a}^\dagger)$ for other types of Lie groups. Typical examples are spin- s , Bloch, $SU(2)$ or atomic CS, whose properties were studied by Radcliffe [16], Gilmore [13, 14] and Perelomov [15]. Also, the concept of squeezing is closely linked to the non compact $SU(1, 1)$ group. In general, there are several definitions or approaches to CS, namely:

1. Barut-Girardello [17]: eigenstates of the annihilation operator.
2. Gilmore-Perelomov: group-theoretical approach [8].
3. Minimal uncertainty and intelligent states [18, 19].
4. Gazeau-Klauder [20]: “non-spreading, temporally stable”, intimately related to a Hamiltonian model.

*Electronic address: rjksama@univ-agadez.edu.ne

†Electronic address: calixto@ugr.es

‡Electronic address: jguerrer@ujaen.es

All definitions are equivalent for canonical CS, but this is not true in general. In this article we shall adopt the Barut-Girardello approach. In particular, we shall deal with special types of nonlinear CS [21] related to the so-called f -oscillator annihilation and creation operators

$$\begin{aligned}\hat{a}_f &= \hat{a}f(\hat{n}) = f(\hat{n}+1)\hat{a} = \sum_{n=0}^{\infty} \sqrt{n+1}f(n+1)|n\rangle\langle n+1| \\ \hat{a}_f^\dagger &= f^\dagger(\hat{n})\hat{a}^\dagger = \hat{a}^\dagger f^\dagger(\hat{n}+1) = \sum_{n=0}^{\infty} \sqrt{n+1}\bar{f}(n+1)|n+1\rangle\langle n|,\end{aligned}\quad (1)$$

where f is an arbitrary function of the number operator $\hat{n} = \hat{a}^\dagger\hat{a}$. Therefore, the nonlinear Hamiltonian $H_f = \omega\hat{a}_f^\dagger\hat{a}_f$ (we use $\hbar = 1$ throughout the article) has eigenvalues $E_n = \omega n|f(n)|^2$, $n = 0, 1, 2, \dots$, (non-equidistant energy levels, in general). This can be interpreted as an amplitude dependent frequency. Nonlinear f -CS $|z, f\rangle$ are then defined as eigenstates of \hat{a}_f , i.e., $\hat{a}_f|z, f\rangle = z|z, f\rangle$, which lead to

$$|z; f\rangle = \mathcal{N}_f^{-\frac{1}{2}}(|z|) \sum_{n=0}^{\infty} \frac{z^n}{\sqrt{n!f(n)!}}|n\rangle, \quad (2)$$

with $f(n)! = f(1)\dots f(n)$, $f(0)! = 1$ and $\mathcal{N}_f(|z|) = \sum_{n=0}^{\infty} \frac{|z|^{2n}}{n!|f(n)!|^2}$ a normalization factor. Nonlinear f -CS are not orthogonal in general, but they form an overcomplete set and close a resolution of the identity [see later on eq. (9) for the hypergeometric case].

On the mathematical side, the general case was studied by Klauder and Penson in [22], where they constructed f -CS and closure relations through solutions of Stieltjes and Hausdorff moment problems (see [23–25] for standard references on the moment problem). They also studied the reverse way, that is, how to define f -CS given a Hamiltonian H with (non necessarily equidistant) spectrum E_n . On the physical side, the first proposal to generate f -CS was given in [26] as emergent stationary states of the motion of an appropriately laser-driven trapped ion. Later, many other generation schemes of f -CS have been explored, for example: single-atom lasers, micromaser under the intensity-dependent Jaynes-Cummings model, excitons in a wide quantum dot, or using a mechanical resonator in an optomechanical microcavity (see e.g [27] and references therein).

In this article we shall restrict ourselves to the special case when $|f(n)|^2$ is a rational function of n , like in Eq. (4). For positive parameters α_j and β_j , these are related to the so called hypergeometric CS [28–30] (HCS for short), of which we make a brief introduction and discuss some representative examples in Section II. We shall not restrict ourselves to positive α_j and β_j , but we shall also consider negative integer cases, for which $|f(n)|^2$ has either zeros or poles. This case leads to “truncated HCS”, of which we also give some interesting examples in Section II B.

CS are said “quasi-classical” and they are used in Quantum Mechanics and Quantum Field Theory to study the classical limit. CS accurately describe the physical properties of many macroscopic quantum systems like in: quantum optics, Bose-Einstein condensates (BEC), superconductors, superfluids, quantum Hall effects, etc. In particular, the ground state of many physical systems undergoing a quantum phase transition is well described by a CS. Actually, it was Gilmore who introduced an algorithm [31], which makes use of CS as variational states to approximate the ground state energy, to study the classical, thermodynamic or mean-field limit of some algebraic quantum models. This algorithm has proved to be specially suitable to analyze the phase diagram of Hamiltonian models undergoing a quantum phase transition like: the Dicke model of atom-field interactions [32, 35, 36, 39], Bose-Einstein condensates [33], the Lipkin-Meshkov-Glick model [34, 37, 38, 40], vibron model for molecules [41–44], bilayer quantum Hall systems [45, 46], etc. In some quantum phases, the ground state is in fact a (parity) symmetry adapted CS or “Schrödinger cat”, $|z, \pm\rangle \propto |z\rangle \pm |-z\rangle$ (even and odd), in the sense of a quantum superposition of two semi-classical (macroscopic) CS with negligible overlap $|\langle z| -z\rangle| \ll 1$ (for large $|z|$), exhibiting squeezing and delocalization, among many other interesting properties. The idea of the even and odd CS was first introduced by Dodonov, Malkin and Man’ko [47, 48] and later extended to more general finite groups than the parity group $\mathbb{Z}_2 = \{1, -1\}$ [48]. Nieto and Traux [49] showed that these states are a special set of nonclassical states and their statistical properties were studied by [50, 51], among many others. Parity-adapted CS were generalized to the nonlinear case of even and odd f -CS [52, 53], their non-classical properties depending on the induced nonlinearity $f(\hat{n})$.

Parity-adapted (even and odd) CS $|z, \pm\rangle$ are also eigenstates of \hat{a}^2 , so that $\hat{a}^2|z, \pm\rangle = z^2|z, \pm\rangle$. The operator \hat{a}^2 plays a fundamental role in creating squeezing, through the squeeze operator $S(\zeta) = \exp[\zeta\hat{a}^2 - \bar{\zeta}\hat{a}^{\dagger 2}]$, and in describing the second harmonic generation (or “frequency doubling”) in nonlinear optics and laser industry. The extension to k -th order harmonic generation and their higher-order squeezing was studied in [54, 55]. Eigenstates of cubic, and higher powers \hat{a}^k , of the annihilation operator lead to generalizations of parity-adapted (even and odd \mathbb{Z}_2) Schrödinger

cat states, sometimes denoted by Schrödinger kittens [9]. However, the k -th order (multiphoton) squeeze operator $S(\zeta) = \exp[\zeta \hat{a}^k - \zeta \hat{a}^{\dagger k}]$ is ill-defined for $k \geq 3$ [56]. These eigenstates of \hat{a}^k can also be written as quantum mechanical superpositions of macroscopically distinguishable CS (finite superpositions of CS first appeared in [57–59]). They can be generated via amplitude dispersion [60, 61] and are used in quantum information processing [62] and quantum spectroscopy [63]. Actually, there is a close relation between eigenstates of \hat{a}^k and the circle representation for CS [64–67], not to be confused with the subject of CS on the circle, of which we comment in appendix A. In particular, in [65] it was proved that standard number eigenstates $|n\rangle$ can be represented as a continuous superposition of CS on the circle. More precisely, denoting $z = re^{i\theta}$, one has

$$|n\rangle = \frac{e^{r^2/2}}{2\pi} \sqrt{n!} r^{-n} \int_0^{2\pi} e^{-in\theta} |re^{i\theta}\rangle d\theta. \quad (3)$$

This equality is just a consequence of the analytical nature of CS and can be extended to all nonlinear CS (Cauchy theorem). Eigenstates of \hat{a}^k can be seen as a discretization of the previous integral and therefore as an approximation to number states $|n\rangle$ by CS superpositions on the circle. This fact was exploited in [68–70] to formulate sampling theorems and discrete Fourier transforms on the sphere, hyperboloid and complex plane, by using the circle representation of $SU(2)$, $SU(1,1)$ and canonical CS. In this article we want to extend all these interesting constructions to general hypergeometric-like CS. Orthonormalized eigenstates of \hat{a}_f^k were introduced by [71], for general f , and some of its statistical properties were discussed in [72]. Here we shall explore many of their interesting properties for f given in (4).

The organization of the paper is as follows. Firstly, in Section II we briefly remind the definition of HCS and their properties, the duality property and the truncation operation when $f(n)$ has either zeros or poles, providing numerous interesting examples. In Section III we introduce the notion of k -hypercats as orthonormalized eigenstates of \hat{a}_f^k and we discuss some of its statistical properties, which reveal that k -hypercats interpolate between number and coherent states. The structure of k -hypercats, as an equally-weighted superposition of HCS uniformly distributed on the circle, suggests a circle representation of number states in terms of HCS on the circle, of which k -hypercats constitute a finite discrete approximation. The case of truncated k -hypercats requires a different definition and they are introduced in Section III D, for which an exact discrete circle representation is possible. In Section IV we generate equally weighted, uniformly distributed on a circle, multicomponent HCS by temporal evolution in a Kerr medium. We corroborate the multicomponent structure by representing the generalized Husimi Q -function [see eq. (50) for a formal definition] in phase space and give a rough estimate for the number of distinguishable components as a function of the standard deviation σ and the initial displacement $|z|$. Finally, Section V is left for conclusions and appendices A, B and C for some clarifications and cumbersome formulas. We also provide a summary table (last page) with numerous interesting examples of hypergeometric CS and their duals.

II. HYPERGEOMETRIC-LIKE CS AND SOME REPRESENTATIVE EXAMPLES

In this article we shall consider the case

$$f(n) = \left(\frac{(\beta_1 + n - 1) \cdots (\beta_q + n - 1)}{(\alpha_1 + n - 1) \cdots (\alpha_p + n - 1)} \right)^{\frac{1}{2}}. \quad (4)$$

For positive α_j and β_j , the nonlinear f -CS of equation (2) are related to the so called HCS [28–30], of which we give a brief in Section II A to set notation and remind their main properties. For negative α_j and/or β_j , the function $f(n)$ has zeros and poles and summations have to be truncated, which implies to deal with finite-dimensional Hilbert spaces (see Section II B for more details).

A. Hypergeometric CS

For f given in (4), we prefer to write nonlinear f -CS (2) as

$$|z; \alpha, \beta\rangle = {}_pF_q(\alpha, \beta; |z|^2)^{-\frac{1}{2}} \sum_{n=0}^{\infty} \frac{z^n}{\sqrt{{}_p\rho_q(n)}} |n\rangle, \quad {}_p\rho_q(n) \equiv n! f(n)!^2. \quad (5)$$

where the normalization function $\mathcal{N}_f(|z|)$ is nothing but the generalized hypergeometric function

$$\mathcal{N}_f(|z|) = {}_pF_q(\alpha, \beta; |z|^2) = \sum_{n=0}^{\infty} \frac{(\alpha_1)_n \cdots (\alpha_p)_n}{(\beta_1)_n \cdots (\beta_q)_n} \frac{|z|^{2n}}{n!}, \quad (6)$$

where $\alpha = (\alpha_1, \dots, \alpha_p)$ and $\beta = (\beta_1, \dots, \beta_q)$ and $(\alpha)_n = \alpha(\alpha+1)\cdots(\alpha+n-1)$, $(\alpha)_0 = 1$ is the Pochhammer-symbol. The series converges for any finite $|z|$ if $p < q + 1$, whereas $p = q + 1$ requires in general $|z| < 1$. The last condition can be relaxed to $|z| = 1$ when $\eta = \Re(\sum_{j=1}^p \alpha_j - \sum_{j=1}^q \beta_j) < 0$ or $0 \leq \eta < 1$ if $z \neq 1$ [28].

Note that hypergeometric f -CS (5) can also be formally written as

$$|z; \alpha, \beta\rangle = {}_pF_q(\alpha, \beta; |z|^2)^{-\frac{1}{2}} {}_pF_q(\alpha, \beta; z\hat{a}^\dagger)|0\rangle, \quad (7)$$

which resembles the usual formula $|z\rangle = \exp(-|z|^2/2) \exp(z\hat{a}^\dagger)|0\rangle$ for canonical CS, replacing the exponential by the hypergeometric function.

Hypergeometric CS are not orthogonal (in general) since

$$\langle z; \alpha, \beta | z'; \alpha, \beta \rangle = \frac{{}_pF_q(\alpha, \beta; \bar{z}z')}{[{}_pF_q(\alpha, \beta; |z|^2) {}_pF_q(\alpha, \beta; |z'|^2)]^{\frac{1}{2}}}, \quad (8)$$

but they form an overcomplete set and close a resolution of the identity

$$\int_{\mathbb{C}} \frac{d^2z}{\pi} {}_p\tilde{\omega}_q(|z|^2) |z; \alpha, \beta\rangle \langle z; \alpha, \beta| = \sum_{n=0}^{\infty} |n\rangle \langle n| = \mathbb{1}, \quad (9)$$

with a weight function ${}_p\tilde{\omega}_q$. Writing ${}_p\omega_q(x) = {}_p\tilde{\omega}_q(x)/{}_pF_q(\alpha, \beta; x)$, with $x = |z|^2$, this function must be a solution of the Hausdorff moment problem

$$\int_0^R {}_p\omega_q(x) x^n dx = {}_p\rho_q(n), \quad x = |z|^2. \quad (10)$$

where $R = 1$ or $R = \infty$. These are classical mathematical problems on which an extensive and mathematically oriented literature exists, see for instance [23–25] and references therein. The solution can be obtained by using Mellin transform techniques [22, 73] and has the form

$${}_p\omega_q(x) = \frac{\Gamma(\alpha_1) \cdots \Gamma(\alpha_p)}{\Gamma(\beta_1) \cdots \Gamma(\beta_q)} G_{p,q+1}^{q+1,0} \left(x \left| \begin{array}{c} \alpha_1 - 1, \dots, \alpha_p - 1 \\ \beta_1 - 1, \dots, \beta_q - 1, 0 \end{array} \right. \right), \quad (11)$$

where G is the Meijer function [74, 75].

Note that although HCS close a resolution of the identity (9), and therefore the P -function for the density operator associated with a HCS is a Dirac delta on \mathbb{C} (as in the case of canonical CS), HCS cannot be considered as classical states, i.e. except for the canonical case ($f(n) = 1$), they possess nonclassical features like non-Poissonian distributions (see Sec. III B), squeezing or anti-bunching (see, for instance, [77]).

A duality transformation was discussed by [76] which, in the case of nonlinear f -CS reduces to $f \rightarrow 1/f$. For f given in (4), this means $p \leftrightarrow q$ and $\alpha \leftrightarrow \beta$. Note that, given a Barut-Girardello eigenstate of \hat{a}_f like (7), it can also be written as a displaced vacuum (an exponential action)

$$|z; \alpha, \beta\rangle = {}_pF_q(\alpha, \beta; |z|^2)^{-\frac{1}{2}} \exp(zf(\hat{n})^{-1}\hat{a}^\dagger)|0\rangle, \quad (12)$$

of the dual nonlinear creation operator $\hat{a}_{1/f}^\dagger = f(\hat{n})^{-1}\hat{a}^\dagger$. In this sense, Barut-Girardello CSs of \hat{a}_f are “exponential” CSs of the dual $\hat{a}_{1/f}$ (in certain cases, when \hat{a}_f and $\hat{a}_{1/f}^\dagger$ close a Lie algebra, they are Gilmore-Perelomov CSs).

Canonical ($p = 0 = q$), $SU(1, 1)$, Susskind-Glogower, etc, CS are recovered as particular cases of HCS. Let us discuss a selection of interesting and paradigmatic cases in more detail, together with their dual cases (see also Table I and II for an account of the most interesting examples of HCS and some of their properties).

1. Barut-Girardello ($p = 0, q = 1, \beta_1 = 2s$) and Perelomov ($p = 1, q = 0, \alpha_1 = 2s$) $SU(1, 1)$ CS.

For the case $p = 0, q = 1, \beta_1 = 2s$, we have that $f(n) = \sqrt{2s + n - 1}$, and therefore $\hat{a}_f = K_-$, where K_- is the annihilation operator of $SU(1, 1)$ algebra:

$$K_- = \sum_{n=0}^{\infty} \sqrt{(n+1)(2s+n)} |n\rangle \langle n+1| \quad (13)$$

The corresponding HCS are:

$$|z; \cdot, 2s\rangle = {}_0F_1(\cdot, 2s; |z|^2)^{-1/2} \sum_{n=0}^{\infty} \left(n! \sqrt{\binom{2s+n-1}{n}} \right)^{-1} z^n |n\rangle, \quad (14)$$

where ${}_0F_1(\cdot, 2s; |z|^2)$ is related to a modified Bessel function, and they are defined on the whole complex plane. These are the original Barut-Girardello CS for $SU(1, 1)$ [17].

The dual case is given $p = 1, q = 0, \alpha_1 = 2s, 1/f(n) = 1/\sqrt{2s+n-1}$, and $\hat{a}_{1/f} = \sum_{n=0}^{\infty} \sqrt{\frac{n+1}{2s+n}} |n\rangle\langle n+1|$. The associated HCS are given by:

$$|z; 2s, \cdot\rangle = (1 - |z|^2)^s \sum_{n=0}^{\infty} \sqrt{\binom{2s+n-1}{n}} z^n |n\rangle. \quad (15)$$

They coincide with Perelomov's coherent states. Note that $\hat{a}_{1/f} \neq K_-$ in this case.

2. Susskind-Glogower ($p = 1, q = 0, \alpha_1 = 1$) and its dual ($p = 0, q = 1, \beta_1 = 1$) CS

Let us study the case $p = 1, q = 0, \alpha_1 = 1$ (Sudarshan harmonius or Susskind-Glogower). For this case $f(n) = \frac{1}{\sqrt{n}}$, thus the annihilation and creation operators are:

$$\hat{a}_f = \sum_{n=0}^{\infty} |n\rangle\langle n+1|, \quad \hat{a}_f^\dagger = \sum_{n=0}^{\infty} |n+1\rangle\langle n|. \quad (16)$$

In this case we recover Susskind-Glogower phase operators [78] $\hat{V} = \hat{a}_f$ and $\hat{V}^\dagger = \hat{a}_f^\dagger$ satisfying $\hat{V}|n\rangle = |n-1\rangle$, $\hat{V}^\dagger|n\rangle = |n+1\rangle$, $n \in \mathbb{N}$ ($\hat{V}|0\rangle = 0$). Susskind-Glogower phase operators satisfy $\hat{V}\hat{V}^\dagger = \mathbb{1}$ and $\hat{V}^\dagger\hat{V} = \mathbb{1} - |0\rangle\langle 0|$. Therefore, these operators are not unitary, but they constitute a partial isometry. They neither close a Lie algebra, since $[\hat{V}, \hat{V}^\dagger] = |0\rangle\langle 0|$. They were introduced in [78] as candidates for quantum phase operators, but there are fundamental issues with the interpretation of these operators (see [79] for an historical review) as quantum phase operators. See Pegg & Barnett [80, 81] for the introduction of new phase operators which solve some of these problems. Nonlinear f -CS for this case lead to

$$|z; 1, \cdot\rangle = \sqrt{1 - |z|^2} \sum_{n=0}^{\infty} z^n |n\rangle. \quad (17)$$

The series is convergent for $|z| < 1$, since the normalization factor is $\mathcal{N}_f(|z|) = \sum_{n=0}^{\infty} |z|^{2n} = \frac{1}{1-|z|^2}$ in this case. These coherent states are true eigenstates of the annihilation operator \hat{V} in this case.

The dual case (in the sense of [76]), $p = 0, q = 1, \beta_1 = 1$, corresponds to $f(n) = \sqrt{n}$ and

$$|z; \cdot, 1\rangle = I_0(2|z|)^{-1/2} \sum_{n=0}^{\infty} \frac{z^n}{n!} |n\rangle, \quad (18)$$

where $I_0(2|z|)$ is the modified Bessel function (see Table I).

The case of CS on the circle [83, 84] could also be seen as a particular case of HCS (namely, $p = 1, q = 0, \alpha_1 = 1$) if we extend the summation in (1,2) to the whole integers (see later on appendix A for more information on this case).

3. Inverse bosonic operator CS ($p = 2, q = 0, \alpha_1 = 1 = \alpha_2$) and Hydrogen-like spectrum ($p = 3, q = 0, \alpha_1 = 1, \alpha_2 = 2 = \alpha_3$)

In [82] inverse bosonic operators are introduced as pseudo-inverses of the usual (either canonical or f -deformed) bosonic operators. It turns out the the inverse of the creation operator acts as an annihilation operator, and therefore Barut-Girardello CS can be defined for it. It is shown that inverse bosonic operators are f -deformed bosonic operators with $f(n) = \frac{1}{nf(n)^*}$.

Inverse bosonic CS for canonical bosonic operators correspond to hypergeometric f -deformed bosonic operators with $p = 2, q = 0, \alpha_1 = 1 = \alpha_2$. Coherent states in this case are ill-defined, since the radius of convergence

is $R = 0$ (see Table I). However, the dual case (in the sense of [76]) is well-defined, corresponding to the case $(p = 0, q = 2, \beta_1 = 1 = \beta_2)$ (see Table I).

Hydrogen-like spectrum $E_n = 1 - \frac{1}{(n+1)^2}$, $n = 0, 1, \dots$, can also be reproduced with an f -deformed oscillator choosing $f(n) = \frac{\sqrt{n+2}}{n+1}$ (see [82]), corresponding to $p = 2, q = 1, \alpha_1 = 2 = \alpha_2, \beta_1 = 3$.

B. Truncated Hypergeometric CS

We shall not restrict ourselves to positive α and β , but we shall also consider negative integer values. In this case, the function $f(n)$ in (4) has poles and zeros that affect the definition of \hat{a}_f , \hat{a}_f^\dagger and $|z; f\rangle$ in (1) and (2). Therefore, for analytic reasons, one must truncate summations in both (1) and (2). The upper limit N of the summation must be chosen as the absolute value of the largest negative α_j or β_j . The normalization factor \mathcal{N}_f is a truncation of the hypergeometric function (6) with absolute values for the Pochhammer symbols

$$\mathcal{N}_f(|z|) = \sum_{n=0}^N \frac{|z|^{2n}}{n!|f(n)!|^2} = \sum_{n=0}^N \frac{|(\alpha_1)_n| \cdots |(\alpha_p)_n| |z|^{2n}}{|(\beta_1)_n| \cdots |(\beta_q)_n| n!}. \quad (19)$$

We can still write this normalization in the form of a truncated hypergeometric function. Indeed, let us denote by ς the number of negative components of α and β . Then $\mathcal{N}_f(|z|) = {}_pF_q(\alpha, \beta; (-1)^\varsigma |z|^2)_N$, the truncated hypergeometric function, where $(-1)^\varsigma$ has been introduced to compensate the negative sign of the Pochhammer symbol, namely $(-|\alpha_j|)_n = (-1)^n (|\alpha_j|)_n$, for $n \leq |\alpha_j|$. This truncation process implies that $|z; f\rangle$ is not an eigenstate of \hat{a}_f anymore, although it can still be considered an ‘‘almost eigenstate’’ for large N in the following sense.

Proposition 1. *The distance from $\hat{a}_f|z; f\rangle$ to $z|z; f\rangle$ is bounded for large N by*

$$\|\hat{a}_f|z; f\rangle - z|z; f\rangle\|^2 < \frac{|z|^{2(N+1)}}{(N!)^{q-p+1}},$$

which tends to zero as $N \rightarrow \infty$ for any $z \in \mathbb{C}$ as long as $q > p - 1$. For $q = p - 1$, $|z| < 1$ is required.

Proof: A direct computation gives

$$\|\hat{a}_f|z; f\rangle - z|z; f\rangle\|^2 = \mathcal{N}_f^{-1}(|z|) \frac{|z|^{2(N+1)}}{N!(f(N)!)^2}.$$

The large N behavior of $f(N)$ in (4) gives $f(N)^2 \sim N^{q-p+1}$, so that $\frac{|z|^{2N}}{N!(f(N)!)^2}$ is smaller and smaller for $q > p - 1$. Since $\mathcal{N}_f(|z|) = 1 + \dots + \frac{|z|^{2N}}{N!(f(N)!)^2}$ (all addends positive), we can say that $\mathcal{N}_f^{-1}(|z|) \frac{|z|^{2(N+1)}}{N!(f(N)!)^2} < \frac{|z|^{2(N+1)}}{N!(f(N)!)^2}$. The rest is a consequence of the Stirling formula. \square

Let us analyze the particular interesting case of $SU(2)$ Barut-Girardello and its dual (Perelomov). Let us consider $p = 0, q = 1, \beta_1 = -2s$. In this case $N = 2s$, and the dimension of the Hilbert space is $2s + 1$. The normalization factor (19) is the hypergeometric function ${}_0F_1(\cdot, -2s; -|z|^2)_{2s}$ truncated to the first $2s + 1$ addends. The nonlinear annihilation operator $\hat{a}_f = i \sum_{n=0}^{2s} \sqrt{(n+1)(2s-n)}|n\rangle\langle n+1|$ coincides with the angular momentum ladder operator iJ_- . As we mentioned before, the truncated HCS

$$|z; \cdot, -2s\rangle = {}_0F_1(\cdot, -2s; -|z|^2)_{2s}^{-1/2} \sum_{n=0}^{2s} \binom{2s}{n}^{-1/2} \frac{(iz)^n}{n!} |n\rangle, \quad (20)$$

is not an eigenstate of J_- , but it is ‘‘almost’’ an eigenstate for large spin s in the sense of the Proposition 1. In this sense, we can denote them as ‘‘almost’’ Barut-Girardello CS for $SU(2)$ and they have been previously introduced by [85]. In [86] and [87] they relate these CS with the Morse potential using Gazeau-Klauder coherent states (see also [88]), although the sum is not up to $N = 2s$ but up to $\nu = s - 1$ for integer s , or $\nu = \lfloor (2s - 1)/2 \rfloor$ for non integer s (in terms of standard floor and ceiling functions), in this case expressing the binomial coefficients and the factorial in terms of the corresponding Gamma functions; the rest of the terms are not present in the spectrum of the Morse potential, as they would correspond to non-normalizable or anti-bound states [89]. The dual case $p = 0, q = 1, \alpha_1 = -2s$ is related to Perelomov spin- s $SU(2)$ CS. Indeed, we recognize the binomial structure of $\hat{a}_f = -i \sum_{n=0}^{2s} \sqrt{(n+1)/(2s-n)}|n\rangle\langle n+1|$. CS

$$|z; -2s, \cdot\rangle = {}_1F_0(-2s, \cdot; -|z|^2)_{2s}^{-1/2} \sum_{n=0}^{2s} \binom{2s}{n}^{1/2} (iz)^n |n\rangle, \quad (21)$$

with ${}_1F_0(-2s, \cdot; -|z|^2)_{2s} = (1 + |z|^2)^{2s}$ the usual Bergman kernel for $SU(2)$.

III. k -TH ORDER NONLINEAR HARMONIC GENERATION AND HYPERGEOMETRIC SCHRÖDINGER KITTENS

In this section we shall compute the eigenstates of \hat{a}_f^k for $k > 1$ and positive α_j and β_j , which appear in the k -th order harmonic generation of nonlinear f -CS. We already know that HCS of equation (5) are eigenstates of \hat{a}_f^k for $k = 1$. For negative α_j and β_j , the truncation process affects the definition of Schrödinger kittens (they are no more eigenstates of \hat{a}_f^k), but an alternative definition can still be considered (see Section IIID).

A. Orthonormalized eigenstates of \hat{a}_f^k and k -hypercats

Now we are interested in the eigenstates of \hat{a}_f^k for $k > 1$. The eigenvalues of \hat{a}_f^k are of the form z^k , and the corresponding eigenspaces are k -fold degenerated, spanned by the HCS $\{|ze^{i\frac{2\pi j}{k}}; \alpha, \beta\rangle, j = 0, 1, \dots, k-1\}$, i. e. HCS with z given by the k -th roots of z^k , and therefore are obtained from $|z; \alpha, \beta\rangle$ by rotating z counter-clock-wise successively by an angle $\frac{2\pi}{k}$. Using eqn. (8), the overlap between these states is given by:

$$G_{jl} = \langle ze^{i\frac{2\pi j}{k}}; \alpha, \beta | ze^{i\frac{2\pi l}{k}}; \alpha, \beta \rangle = \frac{{}_pF_q(\alpha, \beta; |z|^2 e^{i\frac{2\pi(l-j)}{k}})}{{}_pF_q(\alpha, \beta; |z|^2)} \equiv C_{l-j}. \quad (22)$$

This means that these vectors are non-orthogonal. We have the following result:

Proposition 2. *An orthonormalized basis for the eigenspace of eigenstates of \hat{a}_f^k is given by:*

$$|z; \alpha, \beta; k, j\rangle = \frac{1}{k} \left(\frac{{}_pF_q(\alpha, \beta; |z|^2)}{{}_kF_q^j(\alpha, \beta; |z|^2)} \right)^{1/2} \sum_{l=0}^{k-1} e^{-i\frac{2\pi jl}{k}} |ze^{i\frac{2\pi l}{k}}; \alpha, \beta\rangle, \quad j = 0, 1, \dots, k-1. \quad (23)$$

This basis can be rewritten in the usual form:

$$|z; \alpha, \beta; k, j\rangle = {}_kF_q^j(\alpha, \beta; |z|^2)^{-\frac{1}{2}} \sum_{n=0}^{\infty} \frac{z^{nk+j}}{\sqrt{{}_p\rho_q(nk+j)}} |nk+j\rangle, \quad j = 0, 1, \dots, k-1, \quad (24)$$

where ${}_kF_q^j(\alpha, \beta; |z|^2)$ are normalization coefficients (see appendix B for its expression in terms of hypergeometric functions).

Proof: The corresponding Gram matrix G in (22) for the non-orthogonal set $\{|ze^{i\frac{2\pi j}{k}}; \alpha, \beta\rangle, j = 0, 1, \dots, k-1\}$ has a circulant structure (see [68] and references therein), since it depends only on the difference $l-j$. The Gram orthonormalization process is then performed by the Discrete Fourier Transform (DFT) \mathcal{F}_k :

$$|z; \alpha, \beta; k, j\rangle = \lambda_j^{-\frac{1}{2}} \frac{1}{\sqrt{k}} \sum_{l=0}^{k-1} e^{-i\frac{2\pi jl}{k}} |ze^{i\frac{2\pi l}{k}}; \alpha, \beta\rangle, \quad j = 0, 1, \dots, k-1, \quad (25)$$

where $\vec{\lambda} = \sqrt{k}\mathcal{F}_k\vec{C}$ are the eigenvalues of the Gram matrix, which are given by:

$$\begin{aligned} \lambda_j &= \sum_{l=0}^{k-1} e^{-i\frac{2\pi jl}{k}} C_l = \sum_{l=0}^{k-1} e^{-i\frac{2\pi jl}{k}} \frac{{}_pF_q(\alpha, \beta; |z|^2 e^{i\frac{2\pi l}{k}})}{{}_pF_q(\alpha, \beta; |z|^2)} = \frac{1}{{}_pF_q(\alpha, \beta; |z|^2)} \sum_{n=0}^{\infty} \frac{|z|^{2n}}{{}_p\rho_q(n)} \sum_{l=0}^{k-1} e^{-i\frac{2\pi jl}{k}} e^{i\frac{2\pi nl}{k}} \\ &= \frac{k}{{}_pF_q(\alpha, \beta; |z|^2)} \sum_{\nu=0}^{\infty} \frac{|z|^{2(\nu k+j)}}{{}_p\rho_q(\nu k+j)} \equiv k \frac{{}_kF_q^j(\alpha, \beta; |z|^2)}{{}_pF_q(\alpha, \beta; |z|^2)}, \quad j = 0, 1, \dots, k-1, \end{aligned} \quad (26)$$

where we have used the orthogonality relation

$$\sum_{l=0}^{k-1} e^{2\pi i(n-j)l/k} = k\delta_{n,j \bmod k}. \quad (27)$$

With this, the orthonormalized basis (25) is written as (23). Moreover, using an argument similar to that used in (26), the orthonormalized basis also adopts the usual expression (24). The proof does not depend on the fact that we are working with hypergeometric coherent states, and a similar result holds for an arbitrary f (see also [71] for another derivation for arbitrary f). \square

Note that the states (23) have the structure of an equally-weighted superposition of phase-shifted HCS. Therefore, we shall call these states ‘‘hypergeometric Schrödinger kittens’’ or ‘‘ k -hypercats’’ for short, in the sense that they are quantum superpositions of k semi-classical (macroscopic) CS equally distributed on the circle of radius $r = |z|$. The overlap $\langle ze^{2\pi il/k}; \alpha, \beta | ze^{2\pi im/k}; \alpha, \beta \rangle$, $l \neq m$, will be negligible as long as $2\pi|z|/k$ is large enough (see Sec. IV for a quantitative analysis of this distance). The case $k = 2$ is nothing but the even and odd nonlinear CS discussed in [52] for the case of hypergeometric functions f . The particular case $p = q = 0$ (canonical CS) was extensively studied long ago by Jinzuo *et al* [54, 55] and, as we have said, the general f case has been studied by [71, 72], among others. Here we shall further study the properties of these interesting states for the case of hypergeometric f .

The k -hypercats (24) are normalized and orthogonal in the index j (but they are not orthogonal in the index z), and their overlap is given by

$$\langle z; \alpha, \beta; k, j | z'; \alpha, \beta; k, l \rangle = \frac{{}_p^k F_q^j(\alpha, \beta; \bar{z}z')}{[{}_p^k F_q^j(\alpha, \beta; |z|^2) {}_p^k F_q^l(\alpha, \beta; |z'|^2)]^{\frac{1}{2}}} \delta_{jl}. \quad (28)$$

As for HCS, k -hypercats form an overcomplete set and close the resolution of the identity

$$\int_{\mathbb{C}} \frac{d^2 z}{\pi} \sum_{j=0}^{k-1} {}_p^k \omega_q^j(|z|^2) |z; \alpha, \beta; k, j\rangle \langle z; \alpha, \beta; k, j| = \mathbb{1}, \quad (29)$$

where ${}_p^k \omega_q^j(|z|^2) = {}_p \omega_q(|z|^2) {}_p^k F_q^j(\alpha, \beta; |z|^2)$. This closure relation can be easily obtained from (9).

We shall study Canonical and Perelomov $SU(1, 1)$ Schrödinger kittens as representative cases of coherent states on \mathbb{C} and on the unit disk, respectively. For canonical k -cats, the normalization factor in (24) adopts the following form (see [54])

$${}_0^k F_0^j(\cdot, \cdot; |z|^2) = \sum_{l=0}^{k-1} e^{2\pi il(k-j)/k} \exp(|z|^2 e^{2\pi il/k}). \quad (30)$$

For example, for $k = 2$ we have ${}_0^2 F_0^0(\cdot, \cdot; |z|^2) = \cosh(|z|^2)$ and ${}_0^2 F_0^1(\cdot, \cdot; |z|^2) = \sinh(|z|^2)$. For Perelomov $SU(1, 1)$ CS ($p = 1$, $q = 0$, $\alpha_1 = 2s$) we have

$${}_1^k F_0^j(2s, \cdot; |z|^2) = \frac{(2s)_j |z|^{2j}}{j!} {}_{k+1} F_k \left(\frac{2s+j}{k}, \frac{2s+j+1}{k}, \dots, \frac{2s+j+k-1}{k}, 1 \mid |z|^{2k} \right). \quad (31)$$

In particular, for $k = 2$, we have

$${}_1^2 F_0^0(2s, \cdot; |z|^2) = {}_2 F_1 \left(s, s + \frac{1}{2} \mid |z|^4 \right), \quad {}_1^2 F_0^1(2s, \cdot; |z|^2) = {}_2 F_1 \left(s + \frac{1}{2}, s + 1 \mid |z|^4 \right).$$

The special case $s = 1/2$ corresponds to Susskind-Glogower k -cats, which normalization factor adopts the simple form:

$${}_1^k F_0^j(1, \cdot; |z|^2) = \frac{|z|^{2j}}{1 - |z|^{2k}}. \quad (32)$$

B. Statistical properties

Let us now study the photon number statistics of k -hypercats. The probability of detecting m quanta in a k -hypercat $|z; \alpha, \beta; k, l\rangle$ is given by the photon number distribution

$${}_p^k P_q^j(\alpha, \beta; m; |z|^2) = |\langle m | z; \alpha, \beta; k, j \rangle|^2 = {}_p^k F_q^j(\alpha, \beta; |z|^2)^{-1} \frac{|z|^{2m}}{p \rho_q(m)} \delta_{j, m \bmod k}. \quad (33)$$

We shall study, in particular, the two special cases

1. For canonical ($p = 0 = q$) k -cats we have ${}_0^k P_0^j(\cdot, \cdot; m; |z|^2) = \frac{|z|^{2m} \delta_{j, m \bmod k}}{{}_0^k F_0^j(\cdot, \cdot; |z|^2) m!}$

2. For Perelomov $SU(1,1)$ ($p = 1, q = 0, \alpha_1 = 2s$) k -cats we have ${}_1^k P_0^j(2s, \cdot; m; |z|^2) = {}_1^k F_0^j(2s, \cdot; |z|^2)^{-1} \frac{(2s)_m |z|^{2m}}{m!} \delta_{j, m \bmod k}$.

Note that, for the special case $s = 1/2$ (Susskind-Glogower) the probability ${}_1^k P_0^j(1, \cdot, m, |z|^2) = (1 - |z|^{2k}) \delta_{j, m \bmod k}$ does not depend on j .

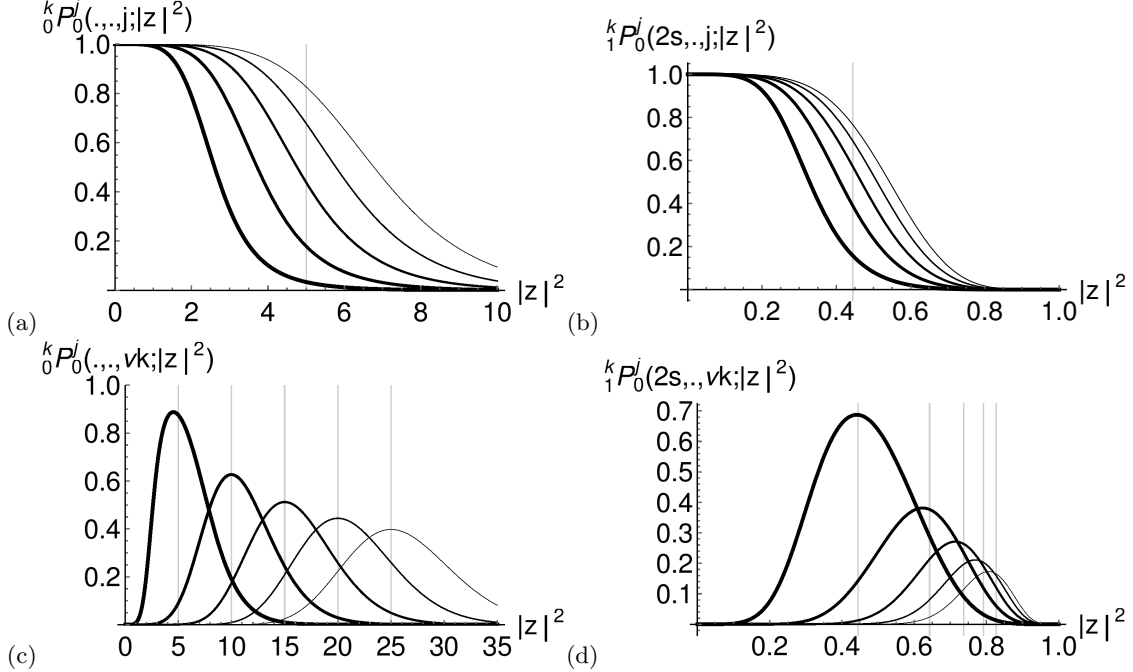


FIG. 1: (Above) Probability ${}_p^k P_q^j(\alpha, \beta; m; |z|^2)$ for: (a) Canonical CS (left, $p = 0 = q$), and (b) Perelomov $SU(1,1)$ (right, $p = 1, q = 0, \alpha_1 = 2s = 6$), for $k = 5$ and $m = j = 0, 1, 2, 3, 4$ (from thickest to thinnest). The critical values of $|z|^2$ are marked with a vertical gridline for canonical, $z_c^2 = k = 5$, and Perelomov $SU(1,1)$, $z_c^2 = (k-1)/(k+2s-2) = 4/9$ CS.

(Below) Probability ${}_p^k P_q^j(\alpha, \beta; m; |z|^2)$ for: (c) Canonical CS (left) and (d) Perelomov $SU(1,1)$ (right), for $k = 5$ and $m = \nu k$ with $\nu = 1, 2, 3, 4, 5$ (from thickest to thinnest). The values of $|z|^2$ where the probabilities have maxima are marked with vertical gridlines for the canonical case, approximately at $|z_{\max}|^2 = \nu k$, and Perelomov $SU(1,1)$, approximately at $z_{\max}^2 = (\nu k - 1)/(\nu k + 2s - 2)$, CS.

The plots in Figure 1 (Above) indicate that ${}_p^k P_q^j(\alpha, \beta; j; |z|^2)$ is close to a step-function $\Theta(|z|^2 - z_c^2) = \begin{cases} 1 & \text{if } |z| < z_c \\ 0 & \text{if } |z| \geq z_c \end{cases}$ for some critical value z_c of $|z|$. That is, for $|z| \ll z_c$, the k -hypercat behaves as a number state $|z; \alpha, \beta; k, j\rangle \simeq |j\rangle$. We can find a representative value of z_c for each k as follows. Consider the projector $\Pi_k = \sum_{n=0}^{k-1} |n\rangle\langle n|$ onto the subspace generated by the first k number states. Take the average $\Pi_k(\alpha, \beta, |z|^2) = \langle \alpha, \beta; z | \Pi_k | \alpha, \beta; z \rangle$ (the operator Π_k symbol). The value of z_c can be obtained as a solution to the saddle point equation $d^2 \Pi_k(\alpha, \beta, x)/dx^2 = 0$. This gives z_c as a function of (k, α, β) . For example, for canonical and Perelomov $SU(1,1)$ cases, we can explicitly compute this critical value, which results in $z_c^2 = k$ and $z_c^2 = (k-1)/(k+2s-2)$, respectively [69, 70]. For the case of Perelomov $SU(1,1)$, this step-function behavior is sharper and sharper for higher values of k and s .

The plots in Figure 1 (Below) indicate that the probabilities ${}_p^k P_q^j(\alpha, \beta; \nu k; |z|^2)$, with $\nu = 1, 2, \dots$ decrease to zero when ν grows, having maxima approximately at $|z_{\max}|^2 = \nu k$ (the larger ν the better approximation) for Canonical CS and approximately at $z_{\max}^2 = (\nu k - 1)/(\nu k + 2s - 2)$ (the smaller ν , the better approximation) for Perelomov $SU(1,1)$ CS.

This behavior indicates that the k -hypercat $|z; \alpha, \beta; k, j\rangle$ is a good approximation of the number state $|j\rangle$ for $|z| \leq z_c$. Let us investigate this fact more closely. For it, let us compute the mean number of photons in a k -hypercat

$$\langle \hat{n} \rangle(\alpha, \beta; k, j; |z|^2) = {}_p^k F_q^j(\alpha, \beta; |z|^2)^{-1} \sum_{n=0}^{\infty} \frac{(nk+j)|z|^{2(nk+j)}}{p \rho_q(nk+j)} = |z|^2 \frac{{}_p^k F_q^{j+k-1}(\alpha, \beta; |z|^2)}{{}_p^k F_q^j(\alpha, \beta; |z|^2)} \quad (34)$$

and the photon number standard deviation

$$\sigma_{\hat{n}}(\alpha, \beta; k, j; |z|^2) = \sqrt{\langle \hat{n}^2 \rangle(\alpha, \beta; k, j; |z|^2) - \langle \hat{n} \rangle(\alpha, \beta; k, j; |z|^2)^2}. \quad (35)$$

By using the fact that, $\hat{n}^2 = \hat{a}^{\dagger 2} \hat{a}^2 + \hat{n}$ and

$$\langle \hat{a}^{\dagger 2} \hat{a}^2 \rangle(\alpha, \beta; k, j; |z|^2) = |z|^4 \frac{{}_k F_q^j(\alpha, \beta; |z|^2)^{-1} d^2}{{}_k F_q^j(\alpha, \beta; |z|^2)} = |z|^4 \frac{{}_k F_q^{j+2k-2}(\alpha, \beta; |z|^2)}{{}_k F_q^j(\alpha, \beta; |z|^2)} \quad (36)$$

we arrive to

$$\sigma_{\hat{n}}(\alpha, \beta; k, j; |z|^2) = \sqrt{|z|^4 \frac{{}_k F_q^{j+2k-2}(\alpha, \beta; |z|^2)}{{}_k F_q^j(\alpha, \beta; |z|^2)} + |z|^2 \frac{{}_k F_q^{j+k-1}(\alpha, \beta; |z|^2)}{{}_k F_q^j(\alpha, \beta; |z|^2)} - \left[|z|^2 \frac{{}_k F_q^{j+k-1}(\alpha, \beta; |z|^2)}{{}_k F_q^j(\alpha, \beta; |z|^2)} \right]^2}. \quad (37)$$

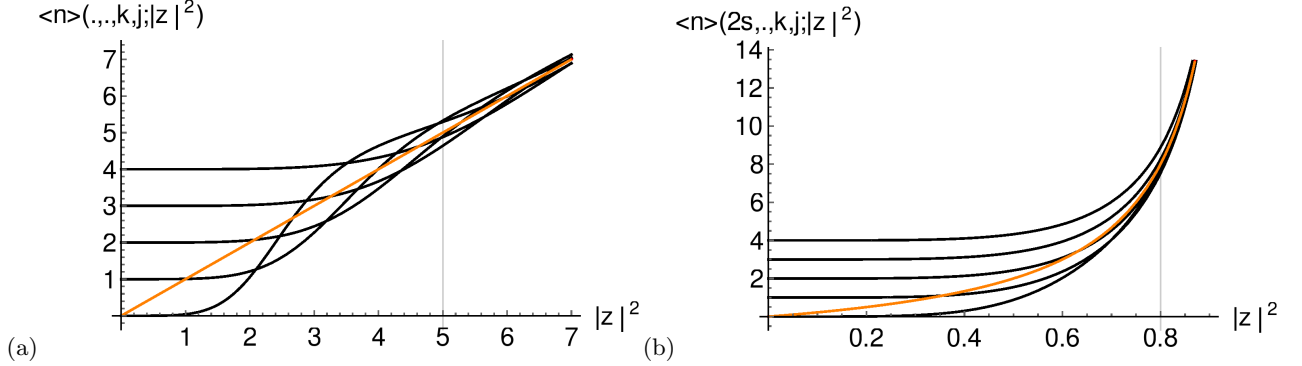


FIG. 2: Mean number $\langle \hat{n} \rangle(\alpha, \beta; k, j; |z|^2)$ of photons for: (a) Canonical CS (left, $p = 0 = q$), and (b) Perelomov $SU(1, 1)$ (right, $p = 1, q = 0, \alpha_1 = 2s = 2$), for $k = 5$ and $j = 0, 1, 2, 3, 4$. In orange we plot the $k = 1$ case, for which $\langle \hat{n} \rangle(\cdot, \cdot; 1, 0; |z|^2) = |z|^2$ and $\langle \hat{n} \rangle(2s, \cdot; 1, 0; |z|^2) = \sqrt{\frac{2sx}{(x-1)^2}}$. Critical values $z_c^2 = 5$ and $z_c^2 = 4/5$ are marked with vertical grid lines.

In Figure 2 we plot the mean number of photons $\langle \hat{n} \rangle(\alpha, \beta; k, j; |z|^2)$ in a k -hypercat $|z; \alpha, \beta; k, j\rangle$ for canonical and Perelomov $SU(1,1)$ cases, as a function of $|z|^2$. We see that, in both cases, the k -hypercat $|z; \alpha, \beta; k, j\rangle$ interpolates between the number state $|j\rangle$, for $|z|^2 \ll z_c^2$, and the CS $|z; \alpha, \beta\rangle$ (the $k = 1$ case), for $|z|^2 \gg z_c^2$ (close to $|z| = 1$ for the $SU(1,1)$ case). Both regions (let us call them: “number and coherent” regions) are separated by a critical value z_c of $|z|$, which depends on k and on α and β . Although we have restricted ourselves to canonical and Perelomov $SU(1,1)$ cases, the general behavior shown in Figure 2 is representative for other values of α and β . In Figure 3 we plot the corresponding photon number standard deviation $\sigma_{\hat{n}}(\alpha, \beta; k, j; |z|^2)$ and we see that whereas it is small in the number region, it grows and approaches the $\sigma_{\hat{n}}(\alpha, \beta)$ (the $k = 1$ CS case) in the CS region. This shows again that $|z; \alpha, \beta; k, j\rangle \simeq |j\rangle$, in the number region, whereas $|z; \alpha, \beta; k, j\rangle \simeq |z; \alpha, \beta\rangle$ in the CS region.

For completeness, let us study deviations from Poissonian distributions for HCSs and its k -hypercats. Since for canonical CS the variance $\sigma_{\hat{n}}$ of the number operator is equal to its average, deviations from Poisson distribution can be measured with the Mandel parameter, defined by the quantity

$$\mathcal{Q} = \frac{\sigma_{\hat{n}}^2 - \langle \hat{n} \rangle}{\langle \hat{n} \rangle} = \mathcal{F} - 1, \quad (38)$$

where $\mathcal{F} = \langle \hat{n}^2 \rangle / \langle \hat{n} \rangle$ is the Fano factor [90]. For $\mathcal{F} < 1$ ($\mathcal{Q} < 0$), the emitted light is referred to as sub-Poissonian, for $\mathcal{F} = 1$, ($\mathcal{Q} = 0$) it corresponds to the Poisson distribution, while for $\mathcal{F} > 1$, ($\mathcal{Q} > 0$) it corresponds to super-Poissonian [91–93]. Let us consider for example the family of confluent ($p = 1 = q$) HCS $|z; \alpha, \beta\rangle = {}_1F_1(\alpha, \beta; |z|^2)^{-\frac{1}{2}} {}_1F_1(\alpha, \beta; z\hat{a}^\dagger)|0\rangle$. Canonical CS are a particular member of this family with $\alpha = \beta$. In Figure 4 we represent the Mandel parameter $\mathcal{Q}(\alpha, \beta, x)$ for confluent hypergeometric CS as a function of $x = |z|^2$ and several values of α, β . We see that for $\alpha < \beta$ the corresponding distribution is super-Poissonian ($\mathcal{Q} > 0$), whereas for $\alpha > \beta$ it is sub-Poissonian ($\mathcal{Q} < 0$), the Poissonian case ($\mathcal{Q} = 0$) being $\alpha = \beta$.

The Mandel parameter for the k -hypercat is explicitly

$$\mathcal{Q}(\alpha, \beta; k, j; x) = x \left(\frac{{}_k F_q^{j+2k-2}(\alpha, \beta; x)}{{}_k F_q^{j+k-1}(\alpha, \beta; x)} - \frac{{}_k F_q^{j+k-1}(\alpha, \beta; x)}{{}_k F_q^j(\alpha, \beta; x)} \right), \quad x = |z|^2. \quad (39)$$

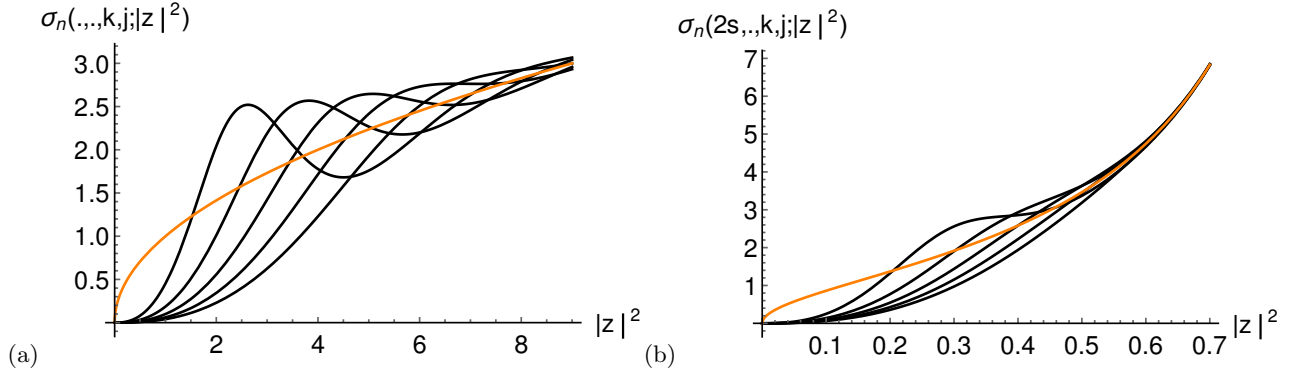


FIG. 3: Photon number standard deviation $\sigma_{\hat{n}}(\alpha, \beta; k, j; |z|^2)$ for: (a) Canonical CS (left, $p = 0 = q$), and (b) Perelomov $SU(1, 1)$ (right, $p = 1, q = 0, \alpha_1 = 2s = 6$), for $k = 5$ and $j = 0, 1, 2, 3, 4$. In orange we plot the $k = 1$ case, for which $\sigma_{\hat{n}}(\cdot, \cdot; 1, 0; |z|^2) = |z|$ and $\sigma_{\hat{n}}(2s, \cdot; 1, 0; |z|^2) = 2s|z|^2/(1 - |z|^2)$.

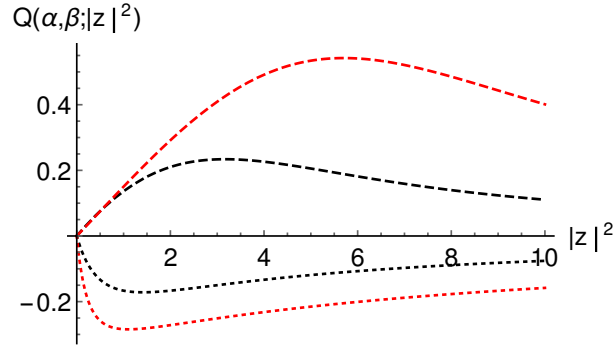


FIG. 4: Mandel parameter $\mathcal{Q}(\alpha, \beta; |z|^2)$ for confluent ($p = 1 = q$) HCS: 1) super-Poissonian $\alpha = 1, \beta = 2$ (dashed black) and $\alpha = 1, \beta = 4$ (dashed red) and 2) sub-Poissonian $\alpha = 2, \beta = 1$ (dotted black) and $\alpha = 4, \beta = 1$ (dotted red).

1. For $f(nk + j) < f(nk + j - 1)$ we have $\mathcal{Q}(\alpha, \beta; k, j; x) > 0$, which yields the super-Poissonian distribution.
2. For $f(nk + j - 1) < f(nk + j)$ we have $\mathcal{Q}(\alpha, \beta; k, j; x) < 0$ which yields the sub-Poissonian distribution.

In Figure 5 we represent the Mandel parameter (39) for confluent ($p = 1 = q$) k -hypercats for the super- sub- and Poissonian cases and $k = 5$. We observe that $\mathcal{Q}(\alpha, \beta; k, 0; 0) = k - 1$ and $\mathcal{Q}(\alpha, \beta; k, j; 0) = -1$ for $j \neq 0$. For large x , $\mathcal{Q}(\alpha, \beta; k, j; x)$ behaves like $\mathcal{Q}(\alpha, \beta, x)$, independently of j for each k .

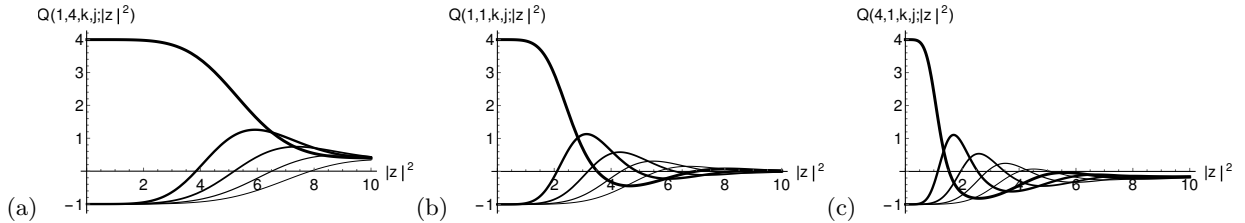


FIG. 5: Mandel parameter $\mathcal{Q}(\alpha, \beta; k, j; |z|^2)$ of $p = 1 = q$ confluent k -hypercats for $k = 5$ and $j = 0, 1, 2, 3, 4$ (from thickest to thinnest curves). We represent (a) Super-Poissonian $\alpha = 1, \beta = 4$, (b) Poissonian $\alpha = 1 = \beta$ and (c) Sub-Poissonian $\alpha = 4, \beta = 1$.

For completeness, in appendix C we also provide formulas for mean values, standard deviations and Mandel parameters for the nonlinear number operator \hat{n}_f . For higher-order squeezing of eigenstates of \hat{a}^k and eigenstates of \hat{a}_f^k we address the reader to Refs. [55] and [72], respectively.

The previous study indicates that the k -hypercatt $|z; \alpha, \beta; k, j\rangle$ constitutes a good approximation to the number

state $|j\rangle$ for high k and small $|z|$. This fact suggests that there must be a circle representation for HCS, like the one in Eq. (3) for canonical CS, the expression (23) being a discrete approximation. Let us study this fact in more detail.

C. The circle representation for hypergeometric CS

A circle representation (3) of basis number states $|n\rangle$ in terms of an equally weighted superposition of canonical CS $|z\rangle$ on the circle of radius $r = |z|$ was proved in [65]. Here we shall provide a variation of this formula but for HCS (5). We shall state this result in the form of a Proposition.

Proposition 3. *A circle representation of basis number states $|n\rangle$ in terms of an equally weighted superposition of HCS $|z; \alpha, \beta\rangle$ on the circle of radius $r = |z|$ is given by*

$$|n\rangle = \sqrt{{}_pF_q(\alpha, \beta; r^2) {}_p\rho_q(n)} \frac{r^{-n}}{2\pi} \int_0^{2\pi} e^{-in\theta} |re^{i\theta}; \alpha, \beta\rangle d\theta. \quad (40)$$

Proof: Just multiply the expression (5) by z^{-m} , integrate on the circle $C = \{z = re^{i\theta}\}$, for fixed radius r , and use the orthogonality property $\int_0^{2\pi} \exp(i\theta(n-m)) d\theta = 2\pi\delta_{n,m}$. \square

In fact, this simple proof is again a consequence of the analytical nature of CS in general. For the present infinite-dimensional case, we can interpret (23) as a finite discretization of (40), in a similar sense to

$$\int_0^{2\pi} g(\theta) d\theta \simeq \frac{2\pi}{k} \sum_{l=0}^{k-1} g(2\pi l/k),$$

for a continuous function g on the circle. The circle representation also applies to the truncated finite-dimensional case. Nevertheless, for the truncated case, a discrete finite exact version of this circle representation exists. Let us discuss it in a separate subsection.

D. Exact finite circle representation for truncated k -hypercats

As we have already noted in Section IIB, HCS $|z; \alpha, \beta\rangle$ for some negative α or β must be truncated [remember the form of the normalization factor in eq. (19)] and, therefore, they are not anymore eigenstates of \hat{a}_f . The same applies for k -hypercats. Nevertheless, we can still define truncated k -hypercats simply by mimicking expression (24) and defining

$$|z; \alpha, \beta; k, j\rangle = {}_pF_q^j(\alpha, \beta; |z|^2)_N^{-\frac{1}{2}} \sum_{n=0}^{(N-k+1)/k} \frac{z^{nk+j}}{\sqrt{{}_p\rho_q(nk+j)}} |nk+j\rangle, \quad j = 0, 1, \dots, k-1, \quad (41)$$

where

$${}_pF_q^j(\alpha, \beta; |z|^2)_N = \sum_{n=0}^{(N-k+1)/k} \frac{|z|^{2(nk+j)}}{|{}_p\rho_q(nk+j)|} \quad (42)$$

is a normalization factor. Remember that N is the absolute value of the largest negative α_j or β_j . Note that now k must be a divisor of $N+1$.

Proposition 4. *The states (41) can also be written as an equally weighted superposition of truncated HCS as*

$$|z; \alpha, \beta; k, j\rangle = \frac{1}{k} \left(\frac{{}_pF_q(\alpha, \beta; (-1)^\sigma |z|^2)_N}{{}_pF_q^j(\alpha, \beta; |z|^2)_N} \right)^{1/2} \sum_{l=0}^{k-1} e^{-2\pi ijl/k} |ze^{2\pi il/k}; \alpha, \beta\rangle, \quad j = 0, 1, \dots, k-1. \quad (43)$$

Therefore, we shall call these states “truncated hypergeometric Schrödinger kittens” or “truncated k -hypercats” for short.

Proof: From the definition of truncated HCS in Section II B, we can define phase-shifted truncated HCS as

$$|ze^{2\pi il/k}; \alpha, \beta\rangle = {}_pF_q(\alpha, \beta; (-1)^\sigma |z|^2)_N^{-\frac{1}{2}} \sum_{n=0}^N \frac{z^n e^{2\pi inl/k}}{\sqrt{{}_p\rho_q(n)}} |n\rangle, \quad l = 0, 1, \dots, k-1. \quad (44)$$

Multiplying both sides by $e^{-2\pi ij l/k}$, summing on l and using the orthogonality condition (27), we arrive to

$$\sum_{l=0}^{k-1} e^{-2\pi ij l/k} |ze^{2\pi il/k}; \alpha, \beta\rangle = {}_pF_q(\alpha, \beta; (-1)^\sigma |z|^2)_N^{-\frac{1}{2}} k \sum_{m=0}^{(N-k+1)/k} \frac{z^{mk+j}}{\sqrt{{}_p\rho_q(mk+j)}} |mk+j\rangle. \quad (45)$$

Comparing the right hand side with (41) we arrive to (43) \square

For $k = N + 1$, the sum in (41) has only one addend ($n = 0$) and therefore $|z; \alpha, \beta; N + 1, j\rangle = |j\rangle$; that is, the truncated $(N + 1)$ -hypercat in (41) coincides with the basis state $|j\rangle$. Therefore, for $k = N + 1$, the expression (43) provides a discrete exact version of the circle representation (40) for truncated HCS. Indeed, we make this explicit in a corollary

Corollary 5. *A discrete exact circle representation of basis number states $|n\rangle$ in terms of an equally weighted superposition of truncated HCS on the circle of radius $r = |z|$ is given by*

$$|n\rangle = \frac{1}{N+1} \left(\frac{{}_pF_q(\alpha, \beta; (-1)^\sigma |z|^2)_N}{{}_p^{N+1}F_q^n(\alpha, \beta; |z|^2)_N} \right)^{1/2} \sum_{l=0}^N e^{-2\pi inl/(N+1)} |ze^{2\pi il/(N+1)}; \alpha, \beta\rangle, \quad n = 0, 1, \dots, N. \quad (46)$$

IV. GENERATING k -HYPERCATS BY AMPLITUDE DISPERSION

As we have previously commented, standard eigenstates of \hat{a}^k are non-classical states of light and can be generated via amplitude dispersion (see [60] for the initial proposal and [61] for recent experiments). To create and manipulate these multi-component Schrödinger cat states, useful in continuous variable quantum information protocols, a strong nonlinear interaction at the single photon level is required. A direct photon-photon interaction occurs in so-called Kerr media (a material whose refractive index depends on the intensity of the light). The anharmonic term in the Hamiltonian is taken to be proportional to \hat{n}^κ , $\kappa > 1$. More precisely, consider an anharmonic oscillator Hamiltonian of the form $H = \hbar\omega\hat{n} + \hbar\Omega\hat{n}^\kappa$, where $\hbar\omega$ is the energy-level splitting for the harmonic part and Ω is the strength of the anharmonic term (Kerr constant). In the interaction picture, an initial CS $|z\rangle$ (describing for example a light beam traveling through such a material) acquires a phase shift $\phi_n(t) = \Omega t n^\kappa$, where t is the interaction time of the light field with the material. Therefore, the revival time is $\tau = 2\pi/\Omega$. Let us see that, at fractions τ/k , the HCS evolves into a equally weighted superposition of HCS on a circle, with a similar structure to the k -hypercat. Indeed, the time evolution of a HCS (5) in the interaction picture is

$$|z, t; \alpha, \beta\rangle = e^{-i\Omega t \hat{n}^\kappa} |z; \alpha, \beta\rangle = {}_pF_q(\alpha, \beta; |z|^2)^{-\frac{1}{2}} \sum_{n=0}^{\infty} \frac{z^n e^{-i\phi_n(t)}}{\sqrt{{}_p\rho_q(n)}} |n\rangle. \quad (47)$$

At fractions $t_k = \tau/k = 2\pi/(\Omega k)$ of the revival time we have $\exp(-i\phi_n(t_k)) = \exp(-2\pi i/k)n^\kappa$; these are powers of the k roots of unity and the sequence is periodic. There are four different cases, according to the parity of κ and k . Let us focus on the case $\kappa = 2$, of which an experiment to engineer an artificial Kerr medium using a three-dimensional circuit quantum electro-dynamic architecture has been done in [61]. For this case, writing $n = n'k + j$, the evolved state (47) at time t_k can be written as a superposition of k -hypercats (24) as

$$|z, t_k; \alpha, \beta\rangle = {}_pF_q(\alpha, \beta; |z|^2)^{-\frac{1}{2}} \sum_{j=0}^{k-1} \sum_{n'=0}^{\infty} \frac{z^{n'k+j} e^{-2\pi ij^2/k}}{\sqrt{{}_p\rho_q(n'k+j)}} |n'k+j\rangle = \sum_{j=0}^{k-1} \frac{{}_pF_q^j(\alpha, \beta; |z|^2)^{\frac{1}{2}}}{{}_pF_q(\alpha, \beta; |z|^2)^{\frac{1}{2}}} e^{-2\pi ij^2/k} |z; \alpha, \beta; k, j\rangle. \quad (48)$$

Now, using the expression (23), we can write the previous state as an equally weighted superposition of HCS on the circle of radius $|z|$ as follows

$$|z, \tau/k; \alpha, \beta\rangle = \frac{1}{k} \sum_{j=0}^{k-1} \sum_{l=0}^{k-1} e^{-2\pi ij(j+l)/k} |ze^{2\pi il/k}; \alpha, \beta\rangle. \quad (49)$$

In order to visualize the structure of this state in phase space, we shall make use of the lower or covariant symbol $Q_{\psi}^{\alpha,\beta}(z) = |\langle \psi | z; \alpha, \beta \rangle|^2$ of the density matrix $\rho = |\psi\rangle\langle\psi|$. This lower symbol coincides with the well known Husimi Q -function for the particular case of $|z; \alpha, \beta\rangle = |z; \cdot, \cdot\rangle$, that is, canonical CS. Then we shall refer to $Q_{\psi}^{\alpha,\beta}(z)$ as “generalized Husimi Q -function”.

In our case, using the HCS overlap (8), the generalized Husimi Q -function of the state $|\psi\rangle = |z_0, \tau/k; \alpha, \beta\rangle$ in (49) is

$$Q_{z_0, k}^{\alpha, \beta}(z) = |\langle z_0, t_k; \alpha, \beta | z; \alpha, \beta \rangle|^2 = \left| \frac{1}{k} \sum_{j=0}^{k-1} \sum_{l=0}^{k-1} \frac{\exp\left(\frac{2\pi i j(j+l)}{k}\right) {}_1F_1(\alpha; \beta; \bar{z}_0 \exp(-\frac{2\pi i l}{k}) z)}{\sqrt{{}_1F_1(\alpha; \beta; |z_0|^2) {}_1F_1(\alpha; \beta; |z|^2)}} \right|^2. \quad (50)$$

Let us have a closer look to the structure of the evolved state $|z_0, \tau/k; \alpha, \beta\rangle$. Note that it can also be written as

$$|z_0, \tau/k; \alpha, \beta\rangle = \frac{1}{k} \sum_{l=0}^{k-1} e^{i\pi \frac{l^2}{2k}} \left(\sum_{j=0}^{k-1} e^{-2\pi i(j+\frac{l}{2})^2/k} \right) |z_0 e^{2\pi i l/k}; \alpha, \beta\rangle. \quad (51)$$

The sum in j can be performed explicitly, and three different cases appear:

- k is odd: All k values of l contribute, therefore there are $m = k$ components in the sum, distributed as the m -th roots of unity multiplied by z_0 .
- k is multiple of 4: Only even values of l contribute, therefore there are $m = k/2$ components in the sum, distributed as the m -th roots of unity multiplied by z_0 .
- k is even but not multiple of 4: Only odd values of l contribute, therefore there are $m = k/2$ components in the sum, distributed as the m -th roots of unity multiplied by z_0 and rotated by $e^{i\frac{2\pi}{k}}$.

In [61] it is commented that to distinguish the m components of a (canonical) kitten, the CSs have to be separated by more than twice their width on a circle with a radius given by the initial displacement $r = |z_0|$. In other words, the coherent states have to be quasi-orthogonal, which means that $2\pi r/m$ has to be large enough. For a canonical CS, the standard deviation of the Gaussian is $\sigma = 1$ (standard normal distribution). We know that about 99.7% of values drawn from a normal distribution are within three standard deviations (“3- σ rule”), which gives $2\pi r/m \gtrsim 3\sigma$. This means that, for a displacement of $r = |z_0| = 2$, the maximum number of canonical CS that can be distinguished is about $m \approx 4$ (thus $k = 8$). Let us compare the temporal evolution of canonical CS with that of HCS of the same family. For example, we know that the confluent hypergeometric function ${}_1F_1(\alpha, \alpha; |z|^2) = \exp(|z|^2)$ and, therefore, canonical CS is a particular case of $p = 1 = q$ HCS $|z; \alpha, \beta\rangle = {}_1F_1(\alpha, \beta; |z|^2)^{-\frac{1}{2}} {}_1F_1(\alpha, \beta; z\hat{a}^\dagger)|0\rangle$. Let us consider the same three cases as we did at the end of Section III B, that is: 1) Poissonian $\alpha = \beta$, 2) Super-Poissonian $\alpha < \beta$ and 3) Sub-Poissonian $\alpha > \beta$. The corresponding (normalized) probability distributions are $f_{\alpha,\beta}(x) = {}_1F_1(\alpha, \beta; x^2)^{-\frac{1}{2}}/\mathcal{N}_{\alpha,\beta}$, where $\mathcal{N}_{\alpha,\beta} = \int_{-\infty}^{\infty} {}_1F_1(\alpha, \beta; x^2)^{-\frac{1}{2}} dx$ is a normalization factor. The variance (squared standard deviation) is $\sigma_{\alpha,\beta}^2 = \int_{-\infty}^{\infty} x^2 f_{\alpha,\beta}(x) dx$. For example $\sigma_{1,1} = 1, \sigma_{1,3} \simeq 1.32$ and $\sigma_{3,1} \simeq 0.75$. Note that $\sigma_{1,3} > \sigma_{1,1} > \sigma_{3,1}$. Using the rough estimate $m \lesssim 2\pi r/(3\sigma)$ we realize that, for a displacement of $r = 2$, the maximum number of HCS that can be distinguished from the multicomponent hypercat (49) is about $m \approx 5$ (thus $k = 5$ or $k = 10$) for $\sigma_{3,1}$ (sub-Poissonian case) and $m \approx 3$ (thus $k = 3$ or $k = 6$) for $\sigma_{1,3}$ (super-Poissonian). Indeed, in Figure 6 we represent the generalized Husimi Q -function $Q_{z_0, k}^{\alpha,\beta}(z)$ of $|z_0, \tau/k; \alpha, \beta\rangle$ for $k = 1, 15, 8, 6, 5, 4, 3, 2$ and $z_0 = 2$. Let us analyze each case separately:

- For $k = 1$ (first column), the state $|z_0, \tau; \alpha, \beta\rangle$ coincides with the initial state $|z_0; \alpha, \beta\rangle$ (complete revival).
- For $k = 15$ (second column), the number of components $m = 15$ is greater than the three critical values $m \simeq 3, 4$ and 5 for super- sub- and Poissonian cases, respectively, and therefore the 15 components can not be distinguished.
- For $k = 8$ (third column), the $m = 4$ components can be clearly distinguished for the Poissonian and sub-Poissonian states (second and third rows, respectively), but not really for the super-Poissonian state (first row), which requires $m \lesssim 3$.
- For $k = 6$ (fourth column), the $m = 3$ components can be distinguished in the three cases, the sub-Poissonian case improving the Poissonian and super-Poissonian cases. Note the similarities between the cases $k = 6$ (fourth column) and $k = 3$ (seventh column) which, according items a) and c) after (51), the 3 components are distributed as the 3-th roots of unity multiplied by z_0 , the case $k = 6$ being rotated an angle $\pi/3$ with respect to the case $k = 3$.

- For $k = 5$ (fifth column), the $m = 5$ components can be distinguished for the sub-Poissonian state, but not really for the Poissonian and super-Poissonian states.
- For $k = 4$ (sixth column), the $m = 2$ components can be distinguished in the three cases.
- Finally, for $k = 2$ the initial state $|z_0; \alpha, \beta\rangle$ goes to the parity reversed $| - z_0; \alpha, \beta\rangle$.

This analysis corroborates the multicomponent structure of the state (51) and the rough estimate $m \lesssim 2\pi r/(3\sigma)$ for the number of distinguishable components as a function of the standard deviation σ and the initial displacement r .

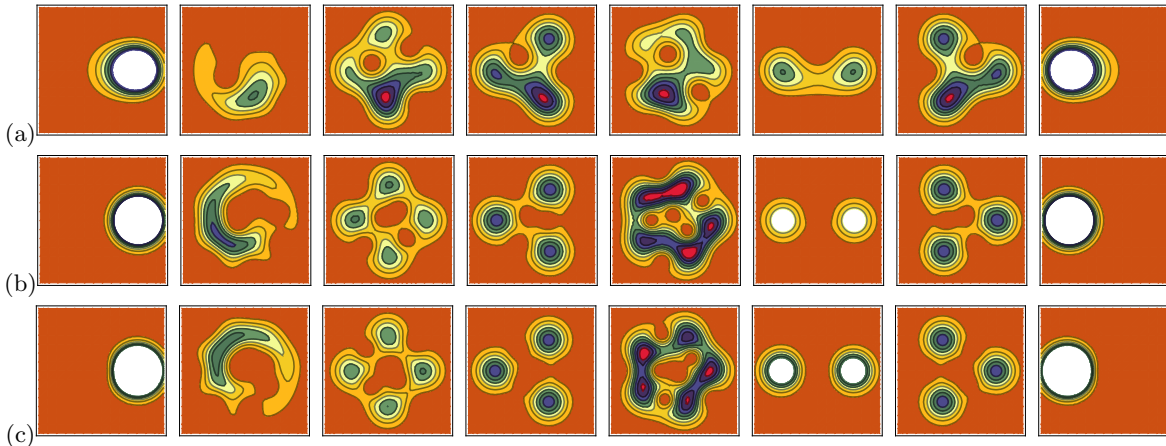


FIG. 6: Contour plots of the generalized Husimi Q -function $Q_{z_0, k}^{\alpha, \beta}(z)$ (50) of the multicomponent state (49) generated by temporal evolution in a Kerr medium from a confluent ($p = 1 = q$) HCS with $z_0 = 2$ at times $t = 0$ and $t_k/\tau = 1/k = 1/15, 1/8, 1/6, 1/5, 1/4, 1/3, 1/2$ (from left to right). The first row (a) corresponds to the super-Poissonian $\alpha = 1, \beta = 3$ case, the second row (b) corresponds to the Poissonian $\alpha = 1, \beta = 1$ case and the third row (c) to the sub-Poissonian case $\alpha = 3, \beta = 1$. We show the window $|x|, |y| \leq 3.5$ for $z = x + iy$.

V. CONCLUSIONS AND OUTLOOK

We have studied mathematical and statistical properties of circular multiphoton CS of hypergeometric type (“ k -hypercats”). They constitute a discrete version of the circle representation and they interpolate between number and coherent states, with a critical displacement z_0 separating the number from de CS region/behavior. These macroscopic equally-weighted superpositions of quantum states (also known as multicomponent Schrödinger cat states, generalizing the usual two-component, even/odd Schrödinger cats) exhibit interesting non-classical properties and can be generated by amplitude dispersion in a Kerr medium. We analyzed the structure in phase space of their generalized Husimi Q -function in the super- and sub-Poissonian cases at different fractions of the revival time. This analysis corroborates their multicomponent structure.

Actual quantum technologies allow to physically realize different kinds of nonlinear f -CS and their quantum superpositions. Since the initial laser-driven trapped ion proposal [26], many more generation schemes have been explored. The literature is huge and we address the reader to, for example, Ref. [27] for the generation of f -CS of the mechanical resonator in an optomechanical microcavity, and references therein on other generation schemes. Of special interest are actual generation schemes inspired in two-dimensional (Dirac-like) materials like graphene, in particular, the use of nanomechanical graphene resonators to prepare vibrational quantum states [94] and to generate macroscopic superposition states [95]. The mathematical construction of Barut-Girardello graphene CS has been recently studied in [96]. The extension to other two-dimensional allotropes (like silicene, exhibiting topological insulator properties) could introduce some novelties. This is work in progress.

Appendix A: Coherent states on the circle

Let us make a clarification. Do not confuse the circle representation with “CS on the circle”. This case could be seen as an extension of Susskind-Glogower operators (16) by letting n to run on \mathbb{Z} . In this case, we recover the phase

operators for the Euclidean group $E(2)$:

$$\hat{a}_f = \hat{U} = \sum_{n=-\infty}^{\infty} |n\rangle\langle n+1|, \quad \hat{a}_f^\dagger = \hat{U}^\dagger = \sum_{n=-\infty}^{\infty} |n+1\rangle\langle n|, \quad (\text{A1})$$

satisfying $\hat{U}|n\rangle = |n-1\rangle$ and $\hat{U}^\dagger|n\rangle = |n+1\rangle, n \in \mathbb{Z}$. These $E(2)$ phase operators satisfy $\hat{U}\hat{U}^\dagger = \hat{U}^\dagger\hat{U} = \hat{I}$, and therefore they are unitary quantum phase operators. They were introduced by Louisell [83], and further studied in [84]. From the group-theoretical point of view, \hat{U} and \hat{U}^\dagger , which are commuting operators, close a finite-dimensional Lie-algebra with the number operator \hat{n} , the Euclidean algebra $E(2)$. In this context, \hat{n} can be understood as rotations on the circumference $-i\frac{\partial}{\partial\phi}$ and \hat{U}, \hat{U}^\dagger as multiplication by a phase $e^{-i\phi}, e^{i\phi}$. Nonlinear f -CS for this case leads to

$$|z, f\rangle \equiv |e^{-in\phi}\rangle = (2\pi)^{-1/2} \sum_{n=-\infty}^{\infty} e^{-in\phi} |n\rangle \quad (\text{A2})$$

since in this case z is restricted to the circle $|z| = 1$. See [84] for the properties of these states. Note that Pegg & Barnett phase operators are constructed from states obtained by considering a finite sum from $n = 0$ up to N in the previous equation and restricting ϕ to the N th-roots of unity.

Perelomov type coherent states can also be introduced for the case of $E(2)$, but since its representations are not square-integrable [97, 98], different approaches have been used to define suitable coherent states. In [97] (see also [99] for applications on signal processing on the circle) the parameters of the $E(2)$ group are restricted to a cylinder, i.e. the phase space of the circle, and even in this case suitable (admissibility) conditions must be imposed on the fiducial vector. See [100] and [101] for a recent account of these states.

There are other approaches for the definition of coherent states on the circle, which are not related with the Susskind-Glogower operators nor with the $E(2)$ groups, like [67, 102]. See the review [103] for details on these and other families of coherent states on the circle.

Appendix B: Normalization factor of k -hypercats

For $j = 1, 2, \dots, k-1$, the normalization factor

$${}^k F_q^j(\alpha, \beta; x) = \sum_{n=0}^{\infty} \frac{x^{nk+j}}{p\rho_q(nk+j)}, j = 0, 1, 2, \dots, k-1, x = |z|^2$$

has the following expression

$${}^k F_q^j(\alpha, \beta; x) = \frac{(\alpha_1, \alpha_2, \dots, \alpha_p)_j}{(\beta_1, \beta_2, \dots, \beta_q)_j} \frac{x^j}{j!} {}^{pk+1} F_{(q+1)k} \left(\begin{matrix} \Delta_k \left[\frac{\alpha_1+j}{k} \right], \dots, \Delta_k \left[\frac{\alpha_p+j}{k} \right], \Delta_1 [1] \\ \Delta_k \left[\frac{\beta_1+j}{k} \right], \dots, \Delta_k \left[\frac{\beta_q+j}{k} \right], \Delta_k \left[\frac{j+1}{k} \right] \end{matrix} \middle| (xk^{p-q-1})^k \right), \quad (\text{B1})$$

where $\Delta_i \left[\frac{a}{b} \right] = \frac{a}{b}, \frac{a+1}{b}, \dots, \frac{a+i-1}{b}$ and $\Delta_1 [1] = 1$. Indeed

$${}^k F_q^j(\alpha, \beta; x) = \sum_{n=0}^{\infty} \frac{x^{nk+j}}{p\rho_q(nk+j)} = \sum_{n=0}^{\infty} \frac{(\alpha_1, \alpha_2, \dots, \alpha_p)_{nk+j}}{(\beta_1, \beta_2, \dots, \beta_q)_{nk+j}} \frac{x^{nk}}{(nk+j)!}. \quad (\text{B2})$$

Rewriting

$$(nk+j)! = j!(j+1)_{nk} = j!k^{nk} \left(\frac{j+1}{k}, \frac{j+2}{k}, \dots, \frac{j+k}{k} \right)_n, \quad (\text{B3})$$

$$(\alpha_1)_{nk+j} = (\alpha_1)_j (\alpha_1+j)_{nk} = k^{nk} (\alpha_1)_j \left(\frac{\alpha_1+j}{k}, \frac{\alpha_1+j+1}{k}, \dots, \frac{\alpha_1+j+k-1}{k} \right)_n \quad (\text{B4})$$

the expression (B2) takes the form

$${}^k F_q^j(\alpha, \beta; x) = \frac{(\alpha_1, \alpha_2, \dots, \alpha_p)_j}{(\beta_1, \beta_2, \dots, \beta_q)_j} \frac{x^j}{j!} \sum_{n=0}^{\infty} \frac{\left(\frac{\alpha_1+j}{k}, \dots, \frac{\alpha_1+j+k-1}{k}, \dots, \frac{\alpha_p+j}{k}, \dots, \frac{\alpha_p+j+k-1}{k} \right)_n \left[(xk^{p-q-1})^k \right]^n}{\left(\frac{\beta_1+j}{k}, \dots, \frac{\beta_1+j+k-1}{k}, \dots, \frac{\beta_q+j}{k}, \dots, \frac{\beta_q+j+k-1}{k}, \frac{j+1}{k}, \dots, \frac{j+k}{k} \right)_n} \quad (\text{B5})$$

If we multiply and divide by $n!$ inside the sum, then this expression can be written like (B1). Note that for $j = 0$, the normalization factor reduces to

$${}_p^k F_q^0(\alpha, \beta; x) = {}_p^k F_{(q+1)k-1} \left(\Delta_k \left[\frac{\alpha_1}{k} \right], \dots, \Delta_k \left[\frac{\alpha_p}{k} \right] \middle| \Delta_k \left[\frac{\beta_1}{k} \right], \dots, \Delta_k \left[\frac{\beta_q}{k} \right], \Delta_{k-1} \left[\frac{1}{k} \right] \right) (xk^{p-q-1})^k. \quad (\text{B6})$$

Appendix C: Mean values, standard deviations and Mandel parameters of \hat{n}_f in a k -hypercat

For $k \geq 3$, we have

$$\langle \hat{n}_f \rangle(\alpha, \beta; j; |z|^2) = |z|^2 \frac{{}_p^k F_q^{j-1}(\alpha, \beta; |z|^2)}{{}_p^k F_q^j(\alpha, \beta; |z|^2)} \quad (\text{C1})$$

and

$$\sigma_{\hat{n}_f} = \sqrt{|z|^4 \frac{{}_p^k F_q^{j-2}(\alpha, \beta; |z|^2)}{{}_p^k F_q^j(\alpha, \beta; |z|^2)} + |z|^2 \frac{{}_p^k F_q^{j-1}(\alpha, \beta; |z|^2)}{{}_p^k F_q^j(\alpha, \beta; |z|^2)} - \left[|z|^2 \frac{{}_p^k F_q^{j-1}(\alpha, \beta; |z|^2)}{{}_p^k F_q^j(\alpha, \beta; |z|^2)} \right]^2}, \quad (\text{C2})$$

which gives the Mandel parameter

$$\mathcal{Q}_f(\alpha, \beta; k, j; x) = x \left(\frac{{}_p^k F_q^{j-2}(\alpha, \beta; x)}{{}_p^k F_q^{j-1}(\alpha, \beta; x)} - \frac{{}_p^k F_q^{j-1}(\alpha, \beta; x)}{{}_p^k F_q^j(\alpha, \beta; x)} \right), \quad x = |z|^2. \quad (\text{C3})$$

Acknowledgements

SA thanks MC and JG for their hospitality during his stay at the University of Granada where this work was done, and the Coimbra Group for the financial support. This study has been partially financed by the Consejería de Conocimiento, Investigación y Universidad, Junta de Andalucía and European Regional Development Fund (ERDF) under projects with Refs. FQM381 and SOMM17/6105/UGR, and by the Spanish MICINN under project PGC2018-097831-B-I00. JG thanks the Spanish MICINN for financial support (FIS2017-84440-C2-2-P).

-
- [1] E. Schrödinger, Der stetige Übergang von der Mikro-zur Makromechanik, *Naturwissenschaften* **14** (1926) 664-666
 - [2] R. Glauber, Coherent and Incoherent States of the Radiation Field, *Phys. Rev. A* **131** (1963) 2766
 - [3] W. Zhang, D. Feng and R. Gilmore, Coherent states: Theory and some applications, *Rev. Mod. Phys.* **62**, 867 (1990)
 - [4] J. R. Klauder, Coherent states for the hydrogen atom, *J. Phys. A* **29** (1996) L293
 - [5] A. Vourdas, Analytic representations in quantum mechanics, *J. Phys. A* **39** (2006) R65-R141
 - [6] S. Twareque Ali, J-P. Antoine, F. Bagarello and J-P. Gazeau, Special issue on coherent states: mathematical and physical aspects, *J. Phys. A* **45** (2012) 24
 - [7] J. R. Klauder and E. C. G. Sudarshan, *Fundamentals of quantum optics* (W. A. Benjamin Inc., New York, 1968)
 - [8] A. Perelomov, *Generalized Coherent States and Their Applications*, Springer-Verlag (1986)
 - [9] V.V. Dodonov and V.I. Man'ko (Eds.), *Theory of Nonclassical States of Light*, Taylor & Francis (2003)
 - [10] J-P. Gazeau, *Coherent States in Quantum Physics*, Wiley-VCH, Berlin, 2009
 - [11] R. J. Glauber, *Quantum Theory of Optical Coherence. Selected Papers and Lectures*, Wiley-VCH, Weinheim 2007
 - [12] S. T. Ali, J.-P. Antoine and J.-P. Gazeau, *Coherent States, Wavelets and Their Generalizations*, (Springer, New York, 2000, 2nd edition 2013)
 - [13] R. Gilmore, Geometry of symmetrized states, *Ann. Phys. (NY)* **74** (1972) 391-463
 - [14] R. Gilmore, On properties of coherent states, *Rev. Mex. Fis.* **23** (1974) 143-187
 - [15] A. M. Perelomov, Coherent states for arbitrary Lie group, *Comm. Math. Phys.* **26** (1972) 222-236
 - [16] J. M. Radcliffe, Some properties of coherent spin states, *J. Phys. A* **4** (1971) 313-323
 - [17] A. O. Barut and L. Girardello, New "coherent" states associated with non compact groups, *Comm. Math. Phys.* **21** (1971) 41-55
 - [18] C. Aragone, G. Guerri, S. Salamo and J.L. Tani, Intelligent spin states, *J. Phys. A* **7** (1974) L149
 - [19] G. Vanden-Bergh and H. DeMeyer, On the existence of intelligent states associated with the non-compact group SU(1,1), *J. Phys. A* **11** (1978) 1569
 - [20] J.-P. Gazeau and J.R. Klauder, Coherent states for systems with discrete and continuous spectrum, *J. Phys. A* **32** (1999) 123-132
 - [21] VI Man'ko, G Marmo, ECG Sudarshan, F Zaccaria, f-Oscillators and nonlinear coherent states, *Physica Scripta* **55** (1997) 528-541
 - [22] J. R. Klauder, K. A. Penson and J.-M. Sixdeniers, Constructing coherent states through solutions of Stieltjes and Hausdorff moment problems, *Phys. Rev. A* **64** (2001) 013817
 - [23] N. I. Akhiezer, *The Classical Moment Problem and Some Related Questions in Analysis*, (Oliver and Boyd, London, 1965)
 - [24] J. D. Tamarkin and J. A. Shohat, *The Problem of Moments*, (APS, New York, 1943)
 - [25] B. Simon, The Classical Moment Problem as a Self-Adjoint Finite Difference Operator, *Adv. Math.* **137** (1998) 82
 - [26] R. L. de Matos Filho and W. Vogel, Nonlinear coherent states, *Phys. Rev. A* **54** (1996) 4560-4563
 - [27] Yan Yan, Jia-pei Zhu and Gao-xiang Li, Preparation of a nonlinear coherent state of the mechanical resonator in an optomechanical microcavity, *Optics Express* **24** (2016) 13590-13609
 - [28] T. Appl and D. H. Schiller, Generalized hypergeometric coherent states, *J. Phys. A* **37** (2004) 2731
 - [29] A Dehghani and B Mojaveri, New nonlinear coherent states based on hypergeometric-type operators, *J. Phys. A* **45** (2012) 095304
 - [30] D. Popov and M. Popov, Some operatorial properties of the generalized hypergeometric coherent states, *Physica Scripta* **90** (2015) 035101(16pp)
 - [31] R. Gilmore, The classical limit of quantum nonspin systems *J. Math. Phys.* **20** (1979) 891-893
 - [32] M. Calixto, Á. Nagy, I. Paradela and E. Romera, Signatures of quantum fluctuations in the Dicke model by means of Rnyi uncertainty, *Phys. Rev. A* **85** (2012) 053813
 - [33] C. Pérez-Campos, J.R. González-Alonso, O. Castaños, R. López-Peña, Entanglement and localization of a two-mode Bose-Einstein condensate, *Ann. Phys. (NY)* **325** (2010) 325-344
 - [34] Lipkin H J, Meshkov N and Glick A J, *Nucl. Phys.* **62**, 188 (1965); *Nucl. Phys.* **62** (1965) 199 ; *Nucl. Phys.* **62** (1965) 211
 - [35] Castaños O., Nahmad-Achar E., Lopez-Peña R. and Hirsch J. G., *Phys. Rev. A* **83** (2011) 051601 ; *Phys. Rev. A* **84** (2011) 013819
 - [36] E. Romera, M. Calixto and Á. Nagy, Entropic uncertainty and the quantum phase transition in the Dicke model, *EPL* **97** (2012) 20011

- [37] O. Castaños, R. López-Peña, J. G. Hirsch and E. López-Moreno, Phase transitions and accidental degeneracy in nonlinear spin systems, *Phys. Rev. B* **72** (2005) 012406
- [38] E. Romera, M. Calixto and O. Castaños, Phase space analysis of first-, second- and third-order quantum phase transitions in the Lipkin-Meshkov-Glick model, *Physica Scripta* **89** (2014) 095103
- [39] R.H. Dicke, Coherence in Spontaneous Radiation Processes, *Phys. Rev.* **93** (1954) 99
- [40] M. Calixto, O. Castaños and E. Romera, Searching for pairing energies in phase space, *EPL* **108** (2014) 47001
- [41] M. Calixto, E. Romera and R. del Real, Parity-symmetry-adapted coherent states and entanglement in quantum phase transitions of vibron models, *J. Phys. A* **45** (2012) 365301(12pp)
- [42] F. Pérez-Bernal and F. Iachello, Algebraic approach to two-dimensional systems: Shape phase transitions, monodromy, and thermodynamic quantities, *Phys. Rev. A* **77** (2008) 032115
- [43] M. Calixto, R. del Real, E. Romera, Husimi distribution and phase-space analysis of a vibron-model quantum phase transition, *Phys. Rev. A* **86** (2012) 032508
- [44] M. Calixto and F. Pérez-Bernal, Entanglement in shape phase transitions of coupled molecular benders, *Phys. Rev. A* **89** (2014) 032126
- [45] Calixto and C. Peón-Nieto, Husimi function and phase-space analysis of bilayer quantum Hall systems at $\nu = 2/\lambda$, *Journal of Statistical Mechanics: Theory and Experiment* (2018) 053112
- [46] M. Calixto, C. Peón-Nieto and E. Pérez-Romero, Hilbert space and ground-state structure of bilayer quantum Hall systems at $\nu = 2/\lambda$, *Phys. Rev. B* **95** (2017) 235302
- [47] V.V. Dodonov, I.A. Malkin and V.I. Man'ko, Even and odd coherent states and excitations of a singular oscillator, *Physica* **72** (1974) 597-615
- [48] O. Castaños, R. Lopez-Peña and V. Man'ko, Crystallized Schrödinger cat states, *J. Russ. Laser Res.* **16** (1995) 477
- [49] M. Nieto and D. Traux, Squeezed states for general systems, *Phys. Rev. Lett.* **71** (1993) 2843
- [50] V. Buzek, A. Viiella-Barranco and P. Knight, Superpositions of coherent states: Squeezing and dissipation, *Phys. Rev. A* **45** (1992) 6750
- [51] M. Hillery, Amplitude-squared squeezing of the electromagnetic field, *Phys. Rev. A* **36** (1987) 3796
- [52] S. Mancini, Even and odd nonlinear coherent states, *Phys. Lett. A* **233** (1997) 291
- [53] S. Sivakumar, *Phys. Lett. A* **250** (1998) 257-262 ; *J. Phys. A* **33** (2000) 2289-2297
- [54] Jinzuo Sun, Jisuo Wang, and Chuankui Wang, Orthonormalized eigenstates of cubic and higher powers of the annihilation operator, *Phys. Rev. A* **44** (1991) 3369-3372
- [55] Jinzuo Sun, Jisuo Wang, and Chuankui Wang, Generation of orthonormalized eigenstates of the operator a^k (for $k \geq 3$) from coherent states and their higher-order squeezing, *Phys. Rev. A* **46** (1992) 1700-1702
- [56] Robert A. Fisher, Michael Martin Nieto and D. Sandberg, Impossibility of naively generalizing squeezed coherent states, *Phys. Rev. D* **29** (1984) 1107-1110 ; Yao-Zhong Zhang, Solving the two-mode squeezed harmonic oscillator and the k th-order harmonic generation in Bargmann-Hilbert spaces, *J. Phys. A* **46** (2013) 455302(13pp)
- [57] U.M. Titulaer and R.J. Glauber, Density operators for coherent states, *Phys. Rev.* **145** (1966) 1041-1050
- [58] Z. Bialynicka-Birula, Properties of the generalized coherent state, *Phys. Rev.* **173** (1968) 1207-1209
- [59] D. Stoler, Generalized coherent states, *Phys. Rev. D* **4** (1971) 2309-2312
- [60] B. Yurke and D. Stoler, Generating Quantum Mechanical Superpositions of Macroscopically Distinguishable States via Amplitude Dispersion, *Phys. Rev. Lett.* **57** (1986) 13-16
- [61] G. Kirchmair et al., Observation of quantum state collapse and revival due to the single-photon Kerr effect, *Nature* **495** (2013) 205-209
- [62] A. Ourjoumtsev, R. Tualle-Brouri, J. Laurat, P. Grangier, Generating Optical Schrödinger Kittens for Quantum Information Processing, *Nature* **312** (2006) 83-86
- [63] M. Kira, S. W. Koch, R. P. Smith, A. E. Hunter and S. T. Cundiff, Quantum spectroscopy with Schrödinger-cat states, *Nature Physics* **7** (2011) 799-804
- [64] J. Janszky, P. Domokos, and P. Adam, Coherent states on a circle and quantum interference, *Phys. Rev. A* **A48** (1993) 2213-2219
- [65] P. Domokos, P. Adam, and J. Janszky, One-dimensional coherent-state representation on a circle in phase space, *Phys. Rev. A* **50** (1994) 4293-4297
- [66] S. Szabo, P. Adam, J. Janszky, and P. Domokos, Construction of quantum states of the radiation field by discrete coherent-state superpositions, *Phys. Rev. A* **53** (1996) 2698-2710
- [67] J.A. González and M.A. del Olmo, Coherent states on the circle and quantization, *J. Phys. A* **31** (1998) 8841-8857
- [68] M. Calixto, J. Guerrero and J.C. Sánchez-Monreal, Sampling Theorem and Discrete Fourier Transform on the Riemann Sphere, *J. Four. Anal. Appl.* **14** (2008) 538-567
- [69] M. Calixto, J. Guerrero, J.C. Sánchez-Monreal, Sampling Theorem and Discrete Fourier Transform on the Hyperboloid, *J. Four. Anal. Appl.* **17** (2011) 240-264
- [70] M. Calixto, J. Guerrero, J.C. Sánchez-Monreal, Almost complete coherent state subsystems and partial reconstruction of wavefunctions in the Fock-Bargmann phase-number representation, *J. Phys. A* **45** (2012) 244029(20pp)
- [71] Xiao-Ming Liu, Orthonormalized eigenstates of $(\hat{a}f(\hat{n}))^k$ ($k \geq 1$) and their generation, *J. Phys. A* **32** (1999) 8685-8689
- [72] Ji-Suo Wang et al. Quantum statistical properties of orthonormalized eigenstates of the operator $(\hat{a}f(\hat{n}))^k$, *J. Phys. B* **35** (2002) 2411-2421
- [73] C. Quesne, Generalized coherent states associated with the C_λ -extended oscillator, *Ann. Phys. (NY)* **293** (2001) 147
- [74] O. I. Marichev, *Handbook of Integral Transforms of Higher Transcendental Functions, Theory and Algorithmic Tables*, (Ellis Harwood, Chichester, 1983).

- [75] I. S. Gradshteyn and I. M. Ryzhik, *Tables of Integrals, Series and Products*, (Academic, New York, 1980).
- [76] S Twareque Ali et al, Representations of coherent states in non-orthogonal bases, *J. Phys. A* **37** (2004) 4407
- [77] K. Zelaya, O. Rosas-Ortiz, Z. Blanco-Garcia and S. Cruz y Cruz, Completeness and nonclassicality of coherent states for generalized oscillator algebras, *Advances in Mathematical Physics* **2017** (2017) 7168592
- [78] L. Susskind and J. Glogower, Quantum mechanical phase and time operator, *Physics* (Long Island City, N.Y.) **1** (1964) 49-61
- [79] M.M. Nieto, Quantum phase and quantum phase operators: some physics and some history *Physica Scripta* **T48** (1993) 5-12
- [80] D.T. Pegg and S.M. Barnett, Unitary Phase Operator in Quantum Mechanics, *Europhys. Lett.* **6** (1988) 483-487
- [81] D.T. Pegg and S.M. Barnett, Phase Properties of the Quantized Single-mode Electromagnetic Field, *Phys. Rev. A* **39** (1989) 1665-1675
- [82] M K Tavassoly, New nonlinear coherent states associated with inverse bosonic and f-deformed ladder operators, *J. Phys. A* **41** (2008) 285305
- [83] W.H. Louisell, Amplitude and phase uncertainty relations, *Phys. Lett.* **7** (1963) 60-61
- [84] R.G. Newton, Quantum action-angle variables for harmonic oscillators, *Ann. Phys. (NY)* **124** (1980) 327
- [85] D. Popov, Spin coherent states defined in the Barut-Girardello manner, *Proceedings of the Romanian Academy, Series A*, **17** (2016) 328-335
- [86] B. Roy and P. Roy, Gazeau-Klauder coherent state for the Morse potential and some of its properties, *Phys. Lett. A* **296** (2002) 187191
- [87] M Angelova and V Hussin, Generalized and Gaussian coherent states for the Morse potential, *J. Phys. A* **41** (2008) 304016
- [88] N. Cotfas, Gazeau-Klauder type coherent states for hypergeometric type operators, *Central European Journal of Physics* **7** (2009) 147-159
- [89] J. Guerrero and V. Aldaya, Inconsistencies in the description of a quantum system with a finite number of bound states by a compact dynamical group, *J. Phys. A* **39** (2006) L267-L276
- [90] J. Bajer and A. Miranowicz, Quantum versus classical descriptions of sub-Poissonian light generation in three-wave mixing, *J. Opt. B* **2** (2000) L10
- [91] L. Mandel, Sub-Poissonian photon statistics in resonance fluorescence, *Opt. Lett.* **4** (1979) 205
- [92] X.-Z. Zhang, Z.-H. Wang, H. Li, Q. Wu, B.-Q. Tang, F. Gao and J.-J. Xu, Characterization of Photon Statistical Properties with Normalized Mandel Parameter, *Chin. Phys. Lett.* **25** (2008) 3976
- [93] J.-P. Antoine, J.-P. Gazeau, P. Monceau, J. R. Klauder and K. A. Penson, Temporally stable coherent states for infinite well and Pöschl-Teller potentials, *J. Math. Phys.* **42** (2001) 2349
- [94] M Bagheri Harouni and M Vaseghi, Preparation of vibrational quantum states in nanomechanical graphene resonator, *Laser Phys.* **26** (2016) 115204
- [95] A. Voje, J. M. Kinaret, and A. Isacson, Generating macroscopic superposition states in nanomechanical graphene resonators, *Phys. Rev. B* **85** (2012) 205415
- [96] Erik Díaz-Bautista and David J. Fernández, Graphene coherent states, *Eur. Phys. J. Plus* **132** (2017) 499
- [97] S. de Bièvre, Coherent states over symplectic homogenous spaces, *J. Math. Phys.* **30** (1989) 1401-1407
- [98] C.J. Isham and J.R. Klauder, Coherent states for n-dimensional Euclidean groups $E(n)$ and their application, *J. Math. Phys.* **32** (1991) 607-620
- [99] B. Torresani, Position-frequency analysis for signals defined on spheres, *Signal Processing* **43** (1995) 341-346
- [100] P.L. García de León and J.P. Gazeau, Coherent state quantization and phase operator, *Phys. Lett. A* **361** (2007) 301-304
- [101] R. Fresneda, J. P. Gazeau and D. Noguera, Quantum localisation on the circle *J. Math. Phys.* **59** (2018) 052105
- [102] S. De Bièvre and J. A. González, in *Quantization and Coherent States Methods*, Proc. XIth Workshop on Geometric Methods in Physics, Białowieza, Poland, 1992, eds. S. Twareque Ali, I. M. Mladenov, and A. Odziejewicz, World Scientific, Singapore, 1993, p. 152.
- [103] H. A. Kastrup, Quantization of the canonically conjugate pair angle and orbital angular momentum, *Phys. Rev. A* **73** (2006) 052104

(p, q)	(α, β)	$f(n)$	\hat{a}_f	$ z; \alpha, \beta\rangle$	$\mathcal{N}_f(z\rangle)$	Domain	Related group	Type	Known as	Dual
$(0, 0)$	(\cdot, \cdot)	1	$\hat{a}_f n\rangle = \sqrt{n} n-1\rangle$	$ z; \cdot, \cdot\rangle = e^{- z ^2/2} \sum_{n=0}^{\infty} \frac{z^n}{\sqrt{n!}} n\rangle$	$e^{ z ^2}$	$z \in \mathbb{C}$	H-W	GP, BG	Canonical CS	Self-dual
$(1, 0)$	$(2s, \cdot)$	$\frac{1}{\sqrt{2s+n-1}}$	$\hat{a}_f n\rangle = \sqrt{\frac{n}{2s+n-1}} n-1\rangle$	$ z; 2s, \cdot\rangle = (1 - z ^2)^s \sum_{n=0}^{\infty} \sqrt{\binom{2s+n-1}{n}} z^n n\rangle$	$(1 - z ^2)^{-2s}$	$ z < 1$	SU(1,1)	GP	GP SU(1,1) CS	BG SU(1,1) CS
$(0, 1)$	$(\cdot, 2s)$	$\sqrt{2s+n-1}$	$\hat{a}_f n\rangle = \sqrt{n(2s+n-1)} n-1\rangle$	$ z; \cdot, 2s\rangle = {}_0F_1(\cdot, 2s; z ^2)^{-1/2} \sum_{n=0}^{\infty} \binom{2s+n-1}{n}^{-1/2} \frac{z^n}{n!} n\rangle$	${}_0F_1(\cdot, 2s; z ^2)$	$z \in \mathbb{C}$	SU(1,1)	BG	BG SU(1,1) CS	GP SU(1,1) CS
$(1, 0)$	$(1, \cdot)$	$\frac{1}{\sqrt{n}}$	$\hat{a}_f n\rangle = n-1\rangle$	$ z; 1, \cdot\rangle = \sqrt{1 - z ^2} \sum_{n=0}^{\infty} z^n n\rangle$	$\frac{1}{1 - z ^2}$	$ z < 1$		BG	Susskind-Glogower CS	Dual SG CS
$(0, 1)$	$(\cdot, 1)$	\sqrt{n}	$\hat{a}_f n\rangle = n n-1\rangle$	$ z; \cdot, 1\rangle = I_0(2 z)^{-1/2} \sum_{n=0}^{\infty} \frac{z^n}{n!} n\rangle$	$I_0(2 z)$	$z \in \mathbb{C}$		BG	Dual SG CS	SG CS
$(2, 0)$	$((1, 1), \cdot)$	$\frac{1}{n}$	$\hat{a}_f n\rangle = \frac{1}{\sqrt{n}} n-1\rangle$	$ z; (1, 1), \cdot\rangle = {}_2F_0((1, 1), \cdot; z ^2)^{-1/2} \sum_{n=0}^{\infty} \sqrt{n!} z^n n\rangle$	${}_2F_0((1, 1), \cdot; z ^2)$	$ z = 0$	H-W		Inverse bosonic CS	Dual Inverse bosonic CS
$(0, 2)$	$(\cdot, (1, 1))$	n	$\hat{a}_f n\rangle = n^{3/2} n-1\rangle$	$ z; \cdot, (1, 1)\rangle = {}_0F_2(\cdot, (1, 1); z ^2)^{-1/2} \sum_{n=0}^{\infty} \frac{z^n}{(n!)^{3/2}} z^n n\rangle$	${}_0F_2(\cdot, (1, 1); z ^2)$	$z \in \mathbb{C}$	H-W		Dual Inverse bosonic CS	Inverse bosonic CS

TABLE I: Hypergeometric CS

(p, q)	(α, β)	$f(n)$	\hat{a}_f	$ z; \alpha, \beta\rangle$	$\mathcal{N}_f(z\rangle)$	Domain	Related group	Type	Known as	Dual
$(0, 1)$	$(\cdot, -2s)$	$\sqrt{(n-2s-1)}$	$\hat{a}_f = i\sqrt{n(n-2s-1)} n-1\rangle$	$ z; \cdot, -2s\rangle = {}_0F_1(\cdot, -2s; - z ^2)_{2s}^{-1/2} \sum_{n=0}^{2s} \binom{2s}{n}^{-1/2} \frac{(iz)^n}{n!} n\rangle$	${}_0F_1(\cdot, -2s; - z ^2)_{2s}$	$z \in \mathbb{C}$	SU(2)	BG	BG SU(2) CS	GP SU(2) CS
$(1, 0)$	$(-2s, \cdot)$	$\frac{1}{\sqrt{n-2s-1}}$	$\hat{a}_f n\rangle = -i\sqrt{n-2s-1} n-1\rangle$	$ z; -2s, \cdot\rangle = (1 + z ^2)^{-s} \sum_{n=0}^{2s} \binom{2s}{n}^{1/2} (iz)^n n\rangle$	$(1 + z ^2)^{2s}$	$z \in \mathbb{C}$	SU(2)	GP	GP SU(2) CS	BG SU(1,1) CS

TABLE II: Truncated Hypergeometric CS